MESTRADO INTEGRADO EM ENGENHARIA QUÍMICA

DESIGN AND DEVELOPMENT OF NOVEL SENSORS FOR BIOLOGICAL AND ENVIRONMENTAL MONITORING

Master's thesis

Developed for the discipline of

Projecto de Desenvolvimento em Instituição Estrangeira

BY

DIANA PAIVA

UMBC
AN HONORS UNIVERSITY IN MARYLAND

CAST
Center for Advanced Sensor Technology

Universidade do Porto
FEUP Faculdade de Engenharia

Departamento de Engenharia Química

JULY 2008

I. Declaration

I hereby declare that the matter embodied in this Thesis is the result of investigation carried out by me in the Center for Advanced Sensor Technology, University of Maryland, Baltimore County, United States of America under supervision of Dr. Ramachandram Badugu and Dr. Leah Tolosa.

In keeping with the general practice of reporting scientific observations due acknowledgements have been made wherever the work described is based on findings of other investigators.

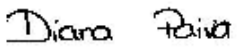

(Diana Paiva)

II. Certificate

Certified that the work contained in the Thesis entitled "Design and Development of Novel Sensors for Biological and Environmental Monitoring" has been carried out by Diana Paiva under our supervision and the same has not been submitted elsewhere for a degree.

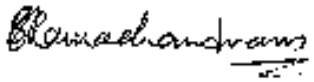

Ramachandram Badugu

(Supervisor)

Leah Tolosa

(Co-supervisor)

Govind Rao

(Director of CAST)

IV. List of Publications

1. Badugu, Ramachamdram; Paiva, Diana; Rao; Govind; Tolosa, Leah. Nitrobenz-oxa-dioazole Labeled Molecularly Imprinted Polymers for the Glutathione Estimation, *manuscript under preparation*.

2. Badugu, Ramachamdram; Paiva, Diana; Rao; Govind; Tolosa, Leah. Development of Metal Ion Sensor Using Small Peptides: Synthesis and Applications, *manuscript under preparation*.

3. Badugu, Ramachamdram; Paiva, Diana; Rao; Govind; Tolosa, Leah. Hg^{2+} Selective NBD Labeled Small Peptide: Synthesis and Applications, *manuscript under preparation*.

4. Badugu, Ramachamdram; Paiva, Diana; Rao; Govind; Tolosa, Leah. Gold Nanoparticles Embedded Molecularly Imprinted Polymers for the Estimation of Cancer Marker, *manuscript under preparation*.

III. Acknowlegements

First I offer my sincerest gratitude to my supervisor, Dr. Ramachandram Badugu, who has supported me throughout my thesis with his patience and knowledge. I attribute the level of my Masters Degree to his encouragement and effort and without him this thesis would not have been completed or written. One simply could not wish for a better or friendlier supervisor. My many thanks also go to my co-supervisor Dr. Leah Tolosa who always being available to provide guidance and discussion whenever it was needed.

The Center for Advanced Sensor Technology led by Prof. Govind Rao at University of Maryland, Baltimore County is also deserving of my appreciation because it gives me the opportunity to do research and develop my scientific skills. I would like to thank all members of CAST group for receiving me, for their support and for their friendship.

I am grateful for everyone that helps me to go a foreign university as exchange student. The opportunity to know a new country, new cultures and different work methods is an amazing experience. Thanks Faculty of Engineering of University of Porto and Department of Chemical Engineering.

Finally and most importantly, I would like to thank my family members and my boyfriend Joaquim Freitas for their support, understanding and patience sustained me to pursue this degree in another country.

IV. Abstract

This thesis has two parts. In the first part we present design and development of molecular imprinted polymers (MIPs) that are useful for the estimation of small molecule markers, such as glutathione, adrenaline and caffeine. The second part of the thesis describes the synthesis and metal sensing properties of two newly designed fluorescence sensors based on small peptides as the recognition element.

At first gold nanoparticles were considered as the signal transducers of analyte binding events of MIPs. For this we prepared near-monodispersed gold nanoparticles. The produced gold nanoparticles embedded MIPs show systematic changes in their absorption spectra in the presence of three analytes studied. Additionally, we have seen more profound and visible color changes of the films in the presence and absence of the analytes. These color changes were quantified using image analysis software to estimate RGB intensity. Observed RGB intensities were changed systematically with increasing concentrations of the analytes.

Subsequently, we explored the feasibility of organic probes as signal transducers. Probes NPM and NBD-Cl were immobilized to the molecular imprinted polymer surface. NBD-Cl was post-grafted on to the polymer surface, whereas the NPM was co-polymerized. MIPs using both of these probes show consistent and expected results. NBD labeled MIP shows high selectivity to its template molecule 3-succinimido)-S-glutathione, (SSG) over several other structurally similar analytes.

For the second part of thesis, we successfully synthesized two new probes using glutathione as the metal recognition moiety. NBD and pyrene derivatives were used as the signaling units. NBD-SG in water with Hg^{2+} shows consistence decrease in fluorescence intensity along with red shift in the band maximum. None other metal ions show any effect on the spectral features of the NBD-SG. Contrary to this NPS-SG shows response to a few metal ions, such as Cr^{3+}, Hg^{2+} and Fe^{3+}. However, its response to Fe^{3+} is more distinguishable.

Keywords

Polymers, Molecular Imprinted Polymers, Nanotechnology, Spectroscopy, Optical Sensors, Gold nanoparticles, glutathione, adrenaline, caffeine, SSG, NPM, NBD-Cl, NBD-SG, NPS-SG, Hg^{2+}, Cr^{3+}, Fe^{3+}, Metal ion sensors, Fluorescence sensors.

V. Contents

VI. Notation and Glossary

Fe^{3+}	Ferric Iron
Hg^{2+}	Mercury
I	Intensity decay
t	Time variable
f_i	Fractional steady-state intensities in a multiexponential intensity decay

Greek Lyrics

λex	Wavelength of excitation
τ_i	Decay time
α_i	Pre-exponential factors in a multiexponential intensity decay
$\bar{\tau}$	Average lifetime
χ^2	Sum of the squared weighted deviations

List of Acronyms

AIBN	2,2'-azobis(isobutyronitrile)
APMAM	*N*-(3-Aminopropyl)methacrylamide hydrochloride
APS	Ammonium persulfate
DMF	Dimethylformamide
DMSO	Dimethylsulfoxide
GSH	Glutathione
ICT	Intermolecular charge transfer
MAA	Methacrylic acid
MBAM	*N*,*N*'-methylenebisacrylamide
MIP	Molecularly Imprinted Polymer
MUA	Mercaptoundecanoic acid
NBD-Cl	4-Chlro-7-nitrobenz-oxa-diazole
NBD-SG	4-(7-nitrobenz-oxa-diazolyl)-*S*-glutathione
NIP	Non-Imprinted Polymer

NIPAM	*N*-isopropyl acrylamide
NPM	*N*-(1-pyrene)maleimide
NPS-SG	3-(*N*-(1-pyrene)succinimido)-*S*-glutathione
PET	Photoinduced inter/intermolecular electron transfer
SSG	3-(succinimido)-*S*-glutathione
TEMED	*N*,*N*,*N*′,*N*′-tetramethylethylenediamine
TOAB	Tetraoctylammonium bromide

1. Introduction

Sensors of any kind are nowadays substantially ubiquitous with the aim of improving the quality of our lives in any technologically advanced applications. Chemical sensors, those sensors transform chemical information into an analytically useful signal, are of particular importance. Among the different chemical sensors, optical sensors offer promising advantages, such as high precision, sensitivity and reproducibility. They are cheap and help developing user-friendly analytical tools. Optical sensors are suitable in monitoring of the analyte concentrations in real-time and real-space. Additionally, these sensors provide high structural feasibility for the development of miniaturized sensor device for bench-top applications. They have, in fact, already found widespread applications in many fields, such as medical diagnosis, environmental monitoring, process control, food and beverage analysis and, lately, toxic gases and explosive detection. It is evident that all these fields are of great importance from a social and economical point of view. The development of sensors seems thus predestined to revolutionize the potentiality of chemical analysis. To this end, since several years, we have been working on the development of low-cost, noninvasive and continuous sensor systems to monitor various analytes (including pH, pO_2, pCO_2, glucose, glutamine etc.) in cell culture. The present project includes two parts; first part describes the development of novel optical sensor material for the estimation of glutathione, adrenaline and caffeine using analyte specific matrix based on molecularly imprinted polymers (MIPs). Whereas the second part portrays the construction and their spectroscopic and analytical features of probes labeled with oligopeptide, glutathione. These newly developed probes show selective response to either ferric ion or mercuric ion. The selectivity of the probe is found to be dependent on the used probe structure. We elaborate these findings in this thesis.

1.1. Molecular imprinted polymers

Development of chemically robust and environmentally stable biomimetic receptor systems capable of binding target molecules with affinities and specificities on a par with natural receptors is a highly active research field. Molecularly imprinting of target analytes in synthetic polymers is one such technique that provides receptors with

high specificities and affinities similar to that of biological receptors [1-9]. Additionally, molecularly imprinted polymers (MIPs) have high stabilities towards extreme environments such as high temperatures and pressures or organic environments, and one can in principle sterilize these materials without adverse effects on their function. Also, the molecular imprinting can be applied to a diverse range of analytes. For example, it is now well established that a wide range of molecular sizes, from small organic molecules to large proteins can be molecularly imprinted [10] and have been used in various applications including, but not limited, in immunoassay-type binding assays [11], chemical sensors [12], as the stationary phases in chromatographic techniques like HPLC [13], chiral separations [14,15], thin-layer chromatography [16], capillary electro-chromatography [17], drug delivery [18] and solid phase extraction [19]. All over the world, scientists are replicating, adapting and evolving synthetic methods for the production of molecularly imprinted polymers in their own laboratories, in order to study and exploit the exquisite molecular recognition properties of these extraordinary materials for their own ends [20].

1.1.1. Polymer synthesis

The constitution of a polymeric substance is usually described in terms of its structural units. These may be defined in the most general terms as groups having a valence of two or more and are connected to one another in polymer molecule by covalent bonds. Properties like high viscosity, long-range elasticity, and high strength are direct consequences of the size and constitution of the polymer structure [21].

Free radical polymerization is the most important synthetic method available today for the conversion of monomer into polymer. This kind of polymerization can be performed under mild reaction conditions (for example, ambient temperatures and atmospheric pressures) in bulk or in solution and are very tolerant of functional groups in the monomers. It is for these reasons, as well as the fact that many monomers are available commercially at low cost, and this method is usually used for preparing molecularly imprinted polymers [20].

The mechanism of free radical polymerization is characterized by three distinct stages: initiation, propagation and termination. For this mechanism it is necessary take special attention in the next two points. First of all, in a typical free radical

polymerization, the rate of propagation is usually much faster than the rate of initiation, such that as soon as a new polymer chain starts to grow it propagates to high molecular weight in a relatively short period of time (perhaps within a second or two) before it terminates. What this means is that high molecular weight product is present in the system even when the amount of monomer consumed is low. Second of all, the source of free radicals (the initiator) is normally active over the entire duration of the polymerization, such that if one were able to take a snap-shot of the system at any given instant time, one would observe the presence of unreacted monomer and initiator, propagating polymer chains and high molecular weight polymer chains that were terminated. Many chemical initiators with different chemical properties can be used as the radical source and normally they are used at low levels compared to the monomer, e.g. 1 wt.%, or 1 mol.% with respect to the total number of moles of monomers [20].

As opposed to a synthesis of homopolymer, as described in the last paragraph, which arises from the polymerization of one single monomer, copolymerization involves the simultaneously polymerization of two or more different monomers. This allows products to be prepared with chemical properties distinct to the polymers obtained upon polymerizing each monomer independently. Particular care must be exercised in free radical copolymerizations to take account of the relative reactivities of the constituent monomers and to appreciate that all monomers are not consumed at the same rate, else the chemical composition of the copolymer products and the distribution of the monomer units within the copolymers may well be dramatically different to what one would predict on the basis of the monomer feed composition alone. It must also be pointed out that for any given pair of comonomers, the molecular composition of the resultant copolymer and the distribution of the monomer units within the copolymer are also dependent upon the relative monomer feed concentrations, and that this can vary with time. Fortunately, the relative reactivities of many common monomers are known and have been tabulated, normally in the form of reactivity ratios for given pairs of monomers [20].

All the polymerizations discussed hitherto involve the propagation of polymers derived from monomers with one single polymerisable group, hereafter referred to as mono-functional monomers. Mono-functional monomers normally polymerize to give linear macromolecules that are soluble in chemically compatible solvents. When multi-

functional monomers are polymerized, either on their own or in combination with a comonomer(s), then the outcome is quite different and this allows a number of non-linear polymer architectures of high commercial value. These materials may be soluble or insoluble, and can be conveniently classified as branched macromolecules, microgels and macroscopic networks (Figure 1). Multi-functional monomers are more commonly referred to as cross-linkers, and serve to chemically link two or more linear polymer chains [20].

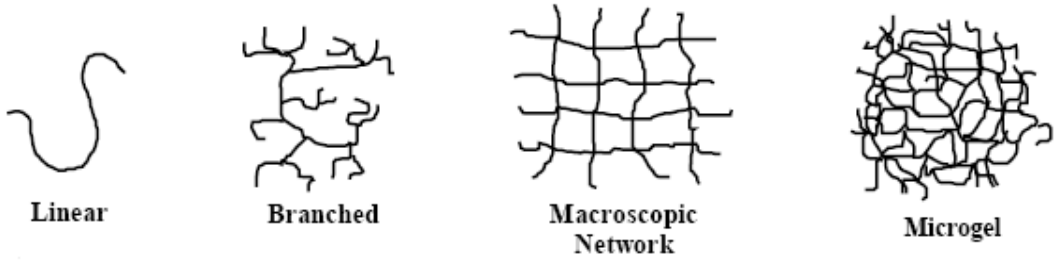

Figure 1: Schematic representation showing polymers with different topologies: linear, branched, macroscopic network and microgel [20].

For the preparation of molecular imprinting materials, macroscopic polymer networks have been, the non-linear polymers, most widely used. As these tend to be insoluble species that lend rigidity and impart mechanical stability to an imprinted binding site. There have been some reports in the literature describing the imprinting of (soluble) microgels and linear macromolecules, but these are relatively few in number [20].

1.1.2. Molecular imprinting in polymers

Molecular imprinting is a process where the functional and cross-linking monomers are copolymerized in the presence of the target analyte (the imprint molecule), which acts as a molecular template. The functional monomers initially form a complex with the imprint molecule. This is then followed by a polymerization step so that the functional groups are held in position by the highly cross-linked polymeric structure. Subsequent removal of the imprint molecule reveals binding sites that are complementary in size and shape to the analyte. One can think of this as introducing 'molecular memory' into the polymer, which is now capable of rebinding the analyte

with a very high specificity [22]. A schematic description of the process is shown in Figure 2.

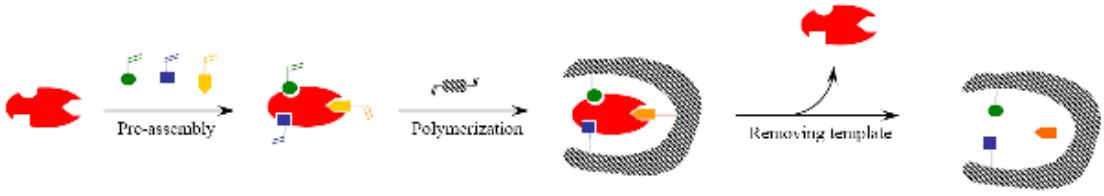

Figure 2: Schematic representation of molecular imprinting process [23].

The type of functional monomer used for producing a useful MIP is very important, as it is the component that is principally involved in forming an effective chemical bond with the print molecule. The functional monomer must strongly interact with the template to achieve a high yield of imprinted binding sites and allow the maximum number of complementary interactions to be developed in the polymeric matrix. In general, analytes containing basic functional groups are best imprinted with monomers containing acid functional groups and vice versa [12].

In an imprinted polymer the cross-linker fulfils three major functions. First of all, the cross-linker is important in controlling the morphology of the polymer matrix, whether it will be gel-type, macroporous or a microgel powder. Secondly, it serves to stabilize the imprinted binding site. Finally, it imparts mechanical stability to the polymer matrix. Much has been written about the effect of the cross-linker on the molecular recognition behavior of imprinted polymers, but from a polymerization point of view, high cross-link ratios are generally preferred in order to access permanently porous (macroporous) materials and in order to be able to generate materials with adequate mechanical stability. Polymers with cross-link ratios in excess of 80% are often the norm [20].

In all molecular imprinting processes the template is of central importance in that it directs the organization of the pendent functional monomers [20]. The binding strength of the polymer as well as the fidelity in the recognition depends on the number and type of interaction sites, the template shape and the monomer template rigidity. Templates offering multiple sites of interactions for the functional monomer are likely to yield binding sites of higher specificity and affinity for the template [12]. Additionally, templates with the susceptibility of reversible covalent bond formation

yield high affinity molecular imprints to their template molecules. In terms of compatibility with free radical polymerization, templates should ideally be chemically inert under the polymerization conditions, thus alternative imprinting strategies may have to be sought if the template can participate in radical reactions or is for any other reason unstable under the polymerization conditions [20].

The choice of the porogenic solvent (*i.e.* the solvent used in the MIP polymerization process) is critical in most molecular imprinting procedures. Porogens govern the strength of noncovalent interactions and influence the polymer morphology such as inner surface area and average pore size. The solvent used in the polymer formation should be as nonpolar as possible in order to maximize the strength of hydrogen and ionic interactions between the print molecule and the monomer while allowing rapid dissolution of the print molecule. The recognition ability of the MIP depends on the type of solvent used in the rebinding step. In general, better recognition ability is obtained with nonpolar solvents. The morphology is also affected by swelling/shrinking when exposed to different kinds of solvents. It is generally observed that the choice of recognition solvent should be more or less identical to the imprinting solvent in order to avoid any swelling problems, which will affect the recognition of the polymer [12].

The vast majority of monomers, especially liquid monomers, are normally supplied with polymerization inhibitor to suppress on-shelf degradation (or self polymerization), and, thus, it is advised to purify the monomers before using in polymerization process. Dissolved oxygen gas in the porogens retards free radical polymerizations, thus in order to maximize the rates of monomer propagation and to, once again, ensure good batch-to-batch reproducibility of polymerizations, removal of the oxygen from monomer solutions immediately prior to polymerization is advisable. Removal of dissolved oxygen can be achieved simply by ultrasonication or by sparging of the monomer solution by an inert gas, e.g. nitrogen or argon [20]. Last but not least, the imprinted polymers are required to wash to remove excessive and bound template to create the MIPs suitable in the analyte binding studies. In some cases, it is reported that the ground imprinted polymers were soxhlet extracted with suitable solvent for several days.

1.1.3. MIPs as optical sensing material

The central part of a chemical or biosensor is the recognition element, which is in close contact with an interrogating transducer. The recognition element is responsible for specifically recognizing and binding the target analyte in an often complex sample. The transducer then translates the chemical signal generated upon analyte binding or conversion into an easily quantifiable output signal [22]. If the target analyte exhibits a special property, this can be exploited for the design of MIP based sensors [22]. If not, it is necessary to incorporate a fluorescent reporter group whose properties are altered upon analyte binding. Accordingly, we used two types of probes, namely plasmonic probes and organic probes for this project.

Plasmonic probes as signal transducers: Noble metallic nanoparticles have been the subject of extensive theoretical and experimental studies [24-26]. These particles exhibit unique and intense color due to incident light induced electronic oscillations in the metallic particles, which is known as so-called plasmon absorption [27,28]. Accordingly, metal nanoparticles show extremely large molar extinction coefficients (~3 x 10^{11} M^{-1} cm^{-1}) equivalent to that of 10^6 fluorophores, and enhanced local electromagnetic fields near the surface of the nanoparticle that are responsible for the intense signals observed in all surface-enhanced spectroscopy [27,28]. Additionally, the plasmon absorption band position and intensity primarily depend on the particle size, shape, composition and nature of the material. It is also known that, the plasmon absorption band shows considerable shift with variations in inter-particle distances and the refractive index of the medium. Both experimental and theoretical studies have shown that the plasmon absorption of proximity coupled nanoparticles is significantly red-shifted from that of the single nanoparticle. The shift decreases approximately exponentially with increasing inter-particles distance to almost zero when the distance between the nanoparticles exceeds ~2.5 times the particle size [29,30]. These unique spectral features have been exploited in various applications including in the development of absorption based colloid proximity sensors for pH [31], DNA [32,33], metal ions [34,35], antibodies [36] and other analytes in solution. In surface immobilized gold colloids, the variations in interparticle distances are minimized but the surface plasmon absorption band of these colloids are predominantly modulated by the change in refractive index of the surrounding medium. This is the principle used in the

construction of surface plasmon resonance optical sensors such as the Biacore system [30].

For this project, the gold colloids will be embedded in a solid polymer matrix that is molecularly imprinted with the glutathione or adrenaline or caffeine as described above. As the analytes bind to the polymer the distances between the gold nanoparticles change thereby modulating the surface plasmon absorption [Figure 3 (A)]. This approach is very similar to that of Matsui et al [37], where a molecularly imprinted polymer with immobilized Au nanoparticles (Au-MIP) was used as a sensing material for adrenaline [37]. The sensing mechanism is based on the variable proximity of the Au nanoparticles immobilized in the imprinted polymer in response to adrenaline binding. As analyte occupies the imprinted binding sites on the polymer the matrix swells causing a blue-shift in the plasmon absorption band of the immobilized Au nanoparticles [Figure 3 (B)]. This combination of molecular imprinting and the Au nanoparticle-based sensing system can be adapted as a general strategy for constructing sensing materials in a tailor-made fashion. The imprinting technique provides the selectivity and sensitivity for the chosen analyte while the proximity coupled gold nanoparticles provides the signal transduction mechanism.

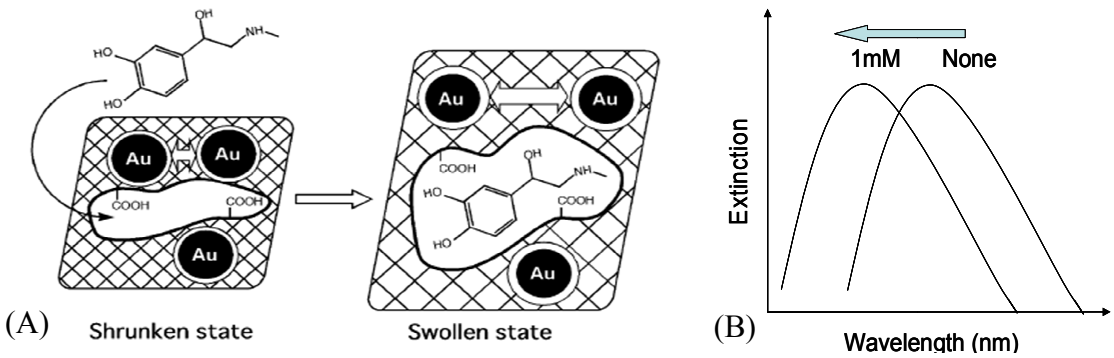

Figure 3: (A) Effect of analyte dependent shrink and swollen states on inter-particle distance [37]; (B) Expected spectral shift associated with increase in inter-particle distance in MIPs.

Organic probes as signal transducers: Apart from using gold nanoparticles as signal transducers of analyte binding events in molecularly imprinted polymers, we considered using several other organic fluorophores as the reporting agents. These provide additional and more sensitive interrogating methods such as fluorescence based techniques. The compounds *N*-(1-pyrene)maleimide (NPM) and 4-amino-7-nitrobenz-

oxa-diazole are a few of these molecules considered for this project. The molecular structures of these probes are depicted in Figure 4. In general, pyrene derivatives such as NPM when in close proximity forms dimers in the excited state and, thus, emit a distinct excimer fluorescence emission. As this phenomenon is proximity-dependent, it is primarily affected by the pyrene concentration. Subsequently, we anticipate that altering the local concentration of the immobilized pyrene derivative (NPM) in the imprinted polymer as the analyte binds to the MIPs can change the monomer-excimer intensity ratio. This is indeed very similar to the inter-particle distance dependent plasmon absorption properties of gold nanoparticles discussed in the last paragraphs.

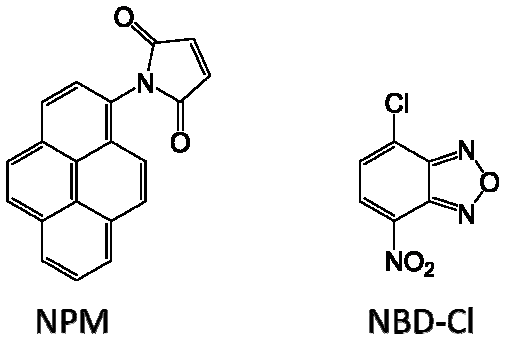

Figure 4: Molecular structures of polymer appendable probes, NPM and NBD-Cl.

Additionally, analyte induced modulations in the MIPs morphology leads to the abrupt changes in the local polarity of the polymer. The fluorescence properties of benzofurazans (for example NBD derivative shown in Figure 4) are highly dependent on solvent polarity. We combine these two characteristics to develop fluorescently labeled MIPs.

1.1.4. Analytes

Glutathione: Glutathione (GSH) is a tripeptide (L-γ-glutamyl-L-cysteinylglycine), which along with other nucleophilic molecules, is believed to protect against the DNA-damaging effects of chemotherapeutic drugs such as cisplatin by conjugating with the toxic moieties in the cytoplasm and preventing them from interacting with the DNA [38,39]. More compelling results, however, suggests that

enhanced DNA repair and increased ability to recover from intracellular toxic events after DNA damage is the more important consequence of GSH [40]. Glutathione S-transferases (GSTs) have been shown to catalyze conjugation of glutathione to a number of chemotherapeutic agents including cisplatin [39,40]. The cisplatin/glutathione conjugate is then ejected out of the cell at the expense of ATP by the membrane-bound multi-drug resistance protein (MRP) [41]. Studies from this group and elsewhere have demonstrated that cellular GSH levels are inversely correlated with cisplatin sensitivity in head and neck cancer cells [42]. For this reason, GSH levels are an indication of the tumor's resistance to the action of chemotherapeutic agents.

GSH concentrations in tissue and plasma have been estimated using a wide variety of techniques, including fluorescence [43,44], colorimetric [45,46] and electrochemical methods [47], among others. Some of these techniques have very low detection limits. For example, the GSH estimation kit available from BioVision shows colorimetric response with ~100 ng/ml (~0,35μM) detection. However, majority of these methods are irreversible, non-continuous, invasive and most importantly require multiple steps prior to the actual measurement. We expected to eliminate these tedious sample preparation steps using high sensitive molecular imprinted polymers.

Adrenaline: Adrenaline is a stress related hormone secreted from adrenal gland, which sits atop of kidneys. When secreted into the bloodstream, it rapidly prepares the body for action in emergency situations. The hormone boosts the supply of oxygen and glucose to the brain and muscles, while suppressing other non-emergency bodily processes (such as digestion in particular). It increases heart rate and stroke volume, dilates the pupils, and constricts arterioles in the skin and gastrointestinal tract while dilating arterioles in skeletal muscles. It elevates the blood sugar level by increasing catabolism of glycogen to glucose in the liver, and at the same time begins the breakdown of lipids in fat cells. Like some other stress hormones, adrenaline has a suppressive effect on the immune system. Estimation of adrenaline has been addressed in early 1950s [48]. Additionally, it is being used as the template in the development of absorption based molecular imprinted polymer by Matsui [37]. We initially, started our project with this molecule as the preliminary data, including polymer composition and conditions for MIPs preparation were available. We exploited these conditions to other analytes used in the present study.

Caffeine: To assess the infiltration of human derived waste and to check for the presence of pharmaceuticals in coastal waters, caffeine was selected as a probe mainly because of its anthropogenic nature, the uniqueness of its origin, its environmental fate, and its elevated consumption. An average person consumes and discards large amounts of caffeine daily. Depending on its origin, freshly brewed coffee contains between 10 to 400 mg/L (parts per million) of caffeine while caffeinated sodas have between 100 and 130 mg/L consequently a single person can generate hundreds to thousands of mg of caffeine per day. The liver extensively metabolizes caffeine and only about 3% leaves the body unmetabolized. Thus, the major source of caffeine in domestic wastewater comes from unconsumed coffee, tea, soft drinks, or medication moving through ineffective on-site wastewater treatment systems (septic tanks). Crowded areas of septic systems present a high risk of microbial fecal contamination to groundwater and general degradation of water quality. Subsequently, considering the importance of understanding the human contamination on aquatic areas, numerous analytical methods have been used in the past. More specifically, caffeine was estimated often from extraction and concentrated samples of known amount of waste water. This methodology is not only time consuming but also in accurate as the methodology depends on the extraction step. Subsequently, avoiding such a tedious concentrating step is critical. In this regard, we anticipate that the caffeine imprinted polymers are suitable candidates for the estimation of caffeine contamination in unprocessed aquatic samples.

1.2. Fluorescence sensors for metal ions

The development of fluorescence sensors capable of selective recognition and sensing of metal ions is one of the most challenging fields from the vantage of organic and supramolecular chemistry. The best effective fluorescence sensor must convert the event of metal ion recognition by the ionophore into light signals over the fluorophore with high sensitivity and ease of monitoring. In designing sensors, therefore, the recognition moiety linked to the fluorophore should be preliminarily considered because they are responsible for the selectivity and binding efficiency of the whole sensors [49]. The second part of this project is focused on the estimation of metal cations such as

mercuric (Hg^{2+}) and ferric (Fe^{3+}) ions using water soluble, probe appended oligopeptide (glutathione) derivatives.

Mercury is an unsafe toxin that has posed a great threat to our environment. Oxidation of mercury vapor in atmosphere to water-soluble Hg^{2+} ions and its consequent metabolism by aquatic microbes produces methyl mercury, which bio-accumulates through the food chain. This is expected to have a severe effect on human health and the environment. The best way to detect Hg^{2+} that has gone into the food chain or contaminated the environment is to monitor the extent of mercury present in microorganisms such as bacteria, which survive in waste water or effluents [50].

On the other hand, iron is one of the most essential metals in the biological systems and plays crucial roles in cellular metabolisms. Especially, ferric iron is widely retained in many proteins and enzymes either for structural purposes or as part of a catalytic site [51]. In order to guarantee adequate ferric iron solubilization and transport into the cells, microorganisms have developed low molecular weight compounds, called siderophores, that are produced when the organism is iron deprived. Siderophores form strong and selective complexes with Fe^{3+} which are usually taken up via membrane receptors. Moreover, deficiencies and excesses of this metal give rise to severe pathologies. Finally, availability of iron seems to be an important factor in determining the stability and composition of aquatic ecosystems [52].

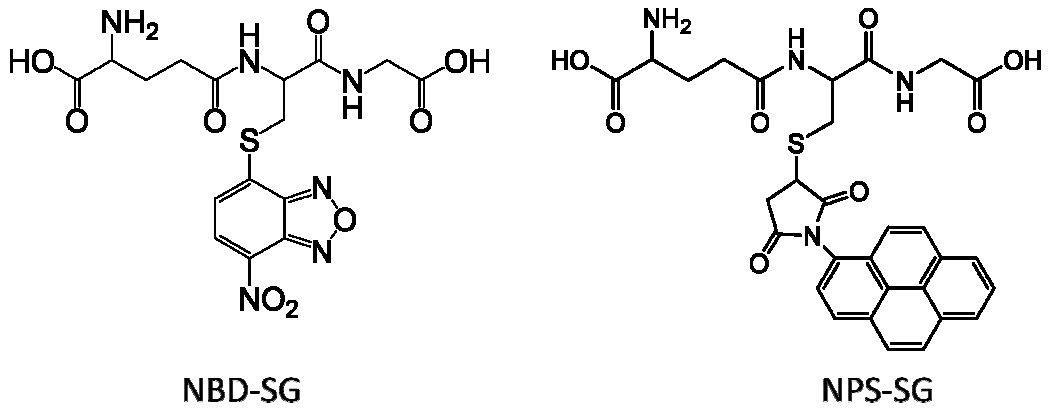

Figure 5: Molecular structures of dye labeled glutathione derivatives, NBD-SG and NPS-SG.

Considering the toxic and biological importance of these metal cations, a great deal of interest is paid to develop iron and mercury selective fluorescence sensors. Here

in this project we developed two new fluorescence sensors using glutathione as the recognizing element and pyrene or nitrobenz-oxa-diazole as the optical signal traducing element. The molecular structures of the developed probes are shown in Figure 5. NBD derivative of glutathione shows Hg^{2+} selectivity, whereas the corresponding pyrene labeled gluthathione derivative shows Fe^{3+} selectivity.

2. Experimental details

2.1. Materials

The following chemicals were used in the present study. *N*-isopropylacrylamide (NIPAM), methacrylic acid (MAA), *N*,*N*'-methylenebisacrylamide (MBAM), 2,2'-azobis(isobutyronitrile) (AIBN), ammonium persulfate (APS), *N*,*N*,*N*′,*N*′-tetramethylethylenediamine (TEMED), acrylamide, *N*-(3-Aminopropyl)methacrylamide hydrochloride (APMAM), 4-Chlro-7-nitrobenz-oxa-diazole (NBD-Cl), *N,N'*-bis(acrylolyl)cystamine, maleimide, glutathione (reduced), glutathione (oxidized), caffeine, adrenaline, tiopronin [N-(2-mercaptopropionyl)glycine], tetraoctylammonium bromide (TOAB), trisodium citrate, sodium tetrachloroaurate ($NaAuCl_4 \bullet 4H_2O$), mercaptoundecanoic acid (MUA), sodium borohydride ($NaBH_4$), 1-aminopyrene, maleic anhydride were purchased from Sigma-Aldrich. HPLC grade, acetonitrile, toluene, chloroform, ethanol, methanol, dimethylformamide (DMF), dimethylsulfoxide (DMSO), ethyl acetate, hexane, ether were obtained from Sigma-Aldrich. Analytical grade acetic acid, nitric acid, sodium acetate, sodium hydroxide, mono- and dipotassium hydrogen phophates, sodium carbonate and sodium bicarbonate were purchased from Sigma-Aldrich. Nanopure water (>18.0 M cm), purified using Millipore Milli-Q gradient system, was used in all experiments.

Buffered solutions (100 mM or 5 mM overall ionic strength) of sodium acetate-acetic acid (for pH range of 1-4), potassium mono and di-basic phosphates (for pH range of 5-8) and sodium carbonate-bicarbonates (for pH range of 9-13) were prepared using standard procedures. The pH of each solution was recorded using a model AR 25 Benchtop/Portable Accumet Research Dual channel pH/ion meter (Fischer Scientific Inc.). The pH adjustments to reach pH 1 and pH 12 and 13 were made with 1N aqueous solutions of HNO_3 and NaOH, respectively. The other buffers were adjusted to whole numbers with corresponding conjugate base or acid.

2.2. Preparation of monolayer-protected gold nanoparticles

To prepare near-monodispersed gold nanoparticles various methods were used depending on solubility in water or organic solvents. Water soluble gold particles were obtained by the treatment of sodium tetrachloroaurate with aqueous trisodium citrate.

Sodium citrate serves as both reducing agent (at refluxing temperatures) and surface protecting ligand. Subsequently, the gold nanoparticles were ligand exchanged with tiopronin [*N*-(2-mercaptopropionyl)glycine]. Tiopronin-protected nanoparticles are stable and readily soluble in aqueous solutions [53].

The gold nanoparticles with sufficient solubility in non-aqueous solutions were prepared by using modified Brust method [54,55], which involves the reduction of the gold salt in dilute two-phase water/toluene solution in the presence of tetraoctylammonium bromide (TOAB). An example procedure is described here. A solution of TOAB (0.825 g, 1.50 mmol) in toluene (100 mL) was added to an aqueous solution of $NaAuCl_4 \bullet 4H_2O$ (3.75 mM, 50 mL, 0.75 mmol). A solution of mercaptoundecanoic acid (MUA) (0.163 g, 0.75 mmol) in toluene (25 mL) was then gradually added to the resulting mixture while vigorously stirring, followed by the dropwise addition of a freshly prepared aqueous solution of $NaBH_4$ (0.30 M, 25 mL, 7.50 mmol). After the mixture was stirred for 1 h, the organic phase was separated and washed with distilled water. The solvent was then completely evaporated in a rotary evaporator and dried in vacuum for 1 day. The obtained black solid was heat treated at 150 °C for 30 min. The heat-treated product was dissolved in 10 mL of toluene, mixed with 200 mL of chloroform to remove the excess unbound TOAB and MUA, and then filtered to give the Au nanoparticles. These nanoparticles are readily soluble in toluene but are sparingly soluble in more polar non-aqueous solvents such as DMSO. Additionally, we also prepared gold nanoparticles without using surface protecting ligand MUA, as described above. These TOAB protected particles in toluene were treated with aqueous tiopronin solution (50 mL, 0.122 g, 0.75 mmol) for about 12 hrs. Subsequently, the organic phase was separated and evaporated in a rotary evaporator. The obtained black solid was heat treated, washed with excess chloroform and filtered to give the Au nanoparticles.

2.3. Preparation of 3-(succinimido)-*S*-glutathione (SSG)

Glutathione contains a free sulfidral (–SH) group that is very reactive with the surface of gold nanoparticles. Thus, it is necessary to change the –SH to a nonreactive form before using it in the molecular imprinting process. For this reason glutathione (reduced) is converted to 3-(succinimido)-*S*-glutathione as shown in Figure 6. The

synthesis involves the reaction of ethanolic solution of glutatathione (0.922 g, 3 mmol) and maleimide (0.291 g, 3 mmol). The reaction mixture in a 50 mL round bottomed flask was stirred at room temperature for 3 hrs. The occurrence of the addition reaction was monitored using silica gel thin layer chromatography (TLC) using ethyl acetate as the eluting solvent. After 3 hrs of stirring no traces of maleimide was observed on the TLC. Subsequently, the solvent ethanol was evaporated to dryness under reduced pressure. The cream colored solid product was purified by washing several times with hexane and ether followed by recrystalization from ethanol.

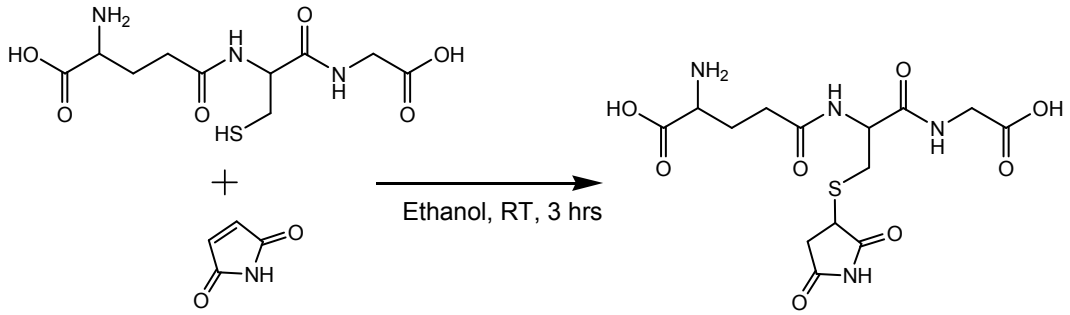

Figure 6: Reaction scheme showing the conversion of glutathione to modified glutathione (SSG).

2.4. Preparation of *N*-(1-pyrene)maleimide (NPM)

NPM was prepared using the following procedure. Compounds 1-aminopyrene (0.217 g, 1 mmol) and maleic anhydride (0.098 g, 1 mmol) were dissolved in 20 mL toluene in a 50 mL round bottom flask equipped with a Dean-Stark apparatus and a reflux condenser. The reaction mixture was refluxed for 6 hrs. The orange solid product was precipitated while cooling the reaction mixture to room temperature. Thus obtained product was filtered and recrystalized from ethanol. The overall yield of the reaction is about 95%.

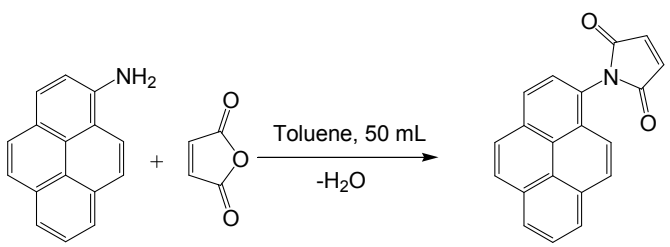

Figure 7: Preparation scheme of NPM.

2.5. Preparation of imprinted and non-imprinted polymers

2.5.1. Gold nanoparticles embedded MIPs and NIPs

The schematic of the molecular imprinting process is shown in Figure 2. Typical polymerization procedure for the preparation of the analyte-imprinted polymer (MIP) with embedded gold nanoparticles involves the polymerization of prepolymer mixture consisting of *N*-isopropylacrylamide (0.480 g, 4.24 mmol, 16%), methacrylic acid (0.030 g, 0.35 mmol, 1%) and *N*,*N*'-methylenebisacrylamide (0.035 g, 0.23 mmol), 2,2'-azobis(isobutyronitrile) (0.150 g, 0.91 mmol) in DMSO (3 mL), including an analyte of interest [3-(succinimido)-*S*-glutathione (SSG) or adrenaline or caffeine (0.23 mmol)] and gold nanoparticles (0.100 g) in a screw capped bottle was first purged with N_2 gas for about 10 min. Subsequently, the above monomers cocktail was heated under a N_2 atmosphere at 70 °C for 3 hrs. Polymers thus obtained were removed from the bottles and washed thoroughly with the solvents in this order: water, methanol, methanol-acetic acid (4:1 v/v) and finally with copious amounts of water. A non-imprinted polymer (NIP) was prepared in the same fashion but without the addition of the analyte. The NIP serves as a reference in all the experiments.

2.5.2. NPM labeled MIPs and NIPs

The synthesis of NPM labeled molecular imprinted and non-imprinted polymers is little different from the imprinting procedure used for the preparation of MIPs and NIPs embedded with gold nanoparticles. Briefly, the NIP and MIPs (imprinted with caffeine or 3-(succinimido)-*S*-glutathione) were prepared from prepolymer mixture of *N*-isopropylacrylamide (16%), metacrylic acid (1%), *N*,*N*'-methylenebisacrylamide (0.020 g), NPM (0.040 g), 2,2'-azobis(isobutyronitrile) (0.050 g) in DMSO (3 mL). At first, the above reaction mixture was vortexed vigorously for about 5 minutes. Subsequently, the mixture was purged with nitrogen gas for about 10 minutes. After the addition of analytes, the mixture was vortexed gently for about a minute before being cast on a cellulosic membrane backing. The backing membrane utilized here is commonly used to filter dairy milk and will be referred to from here on as milk-filter. The milk-filter membrane is held in place between two glass plates with Teflon spacers. Polymerizing between the two glass plates helps keep an oxygen free environment for

the reaction while ensuring a uniform film thickness as determined by the spacers. Free radical polymerization of the acrylate end groups were initiated by the added AIBN at elevated temperature (70ºC). After allowing polymerization to proceed for about 3 hr, the NPM labeled NIP and MIP films now firmly affixed to the milk-filter membrane was peeled off from the glass plates. Thus obtained polymer films were first soaked in water for overnight followed by extensive washing with water, and with methanol and methanol-acetic acid (9:1, v/v). Finally, films were washed under stream of deionized water. The washed films were stored in water until use.

2.5.3. NBD labeled MIPs and NIPs

The synthesis of NBD labeled NIP and MIP is shown in Figure 8. This is little different from the procedure used for NPM labeled ones. Here in this case, we first made the blank NIP and MIP (*i.e.* no NBD dye was added to the prepolymer mixture) films and then the dye NBD is post-doped on to the films. Also, the polymer composition and porogenic solvent used are different. Additionally, a new functional monomer, *N*-(3-aminopropyl)methacrylamide, is added that facilitate free amine groups on the polymer that react with the post-doping dye NBD-Cl. This is briefly, a mixture of *N*-isopropylacrylamide (0.160 g, 1.41 mmol, 8%), acrylamide (0.160 g, 2.25 mmol, 8%), methacrylic acid (0.020 g, 0.23 mmol, 1%), *N*-(3-aminopropyl)methacrylamide hydrochloride (0.020 g, 0.112 mmol, 1%) and *N*,*N*'-methylenebisacrylamide (0.030 g, 0.195 mmol) in water (2 mL), and add 400 µL of 10% aqueous ammonium persulfate solution was purged with nitrogen gas for about 10 minutes. Then we added the template 3-(succinimido)-*S*-glutathione (0.093 g, 0.23 mmol) followed by the addition of 30 µL TEMED. Subsequently, the mixture was vortexed gently before being cast on to milk-filter membrane. After allowing the polymerization to proceed for about 4 hr at room temperature, the NIP and MIP films were washed thoroughly as mentioned previously and soaked in deionized water for overnight.

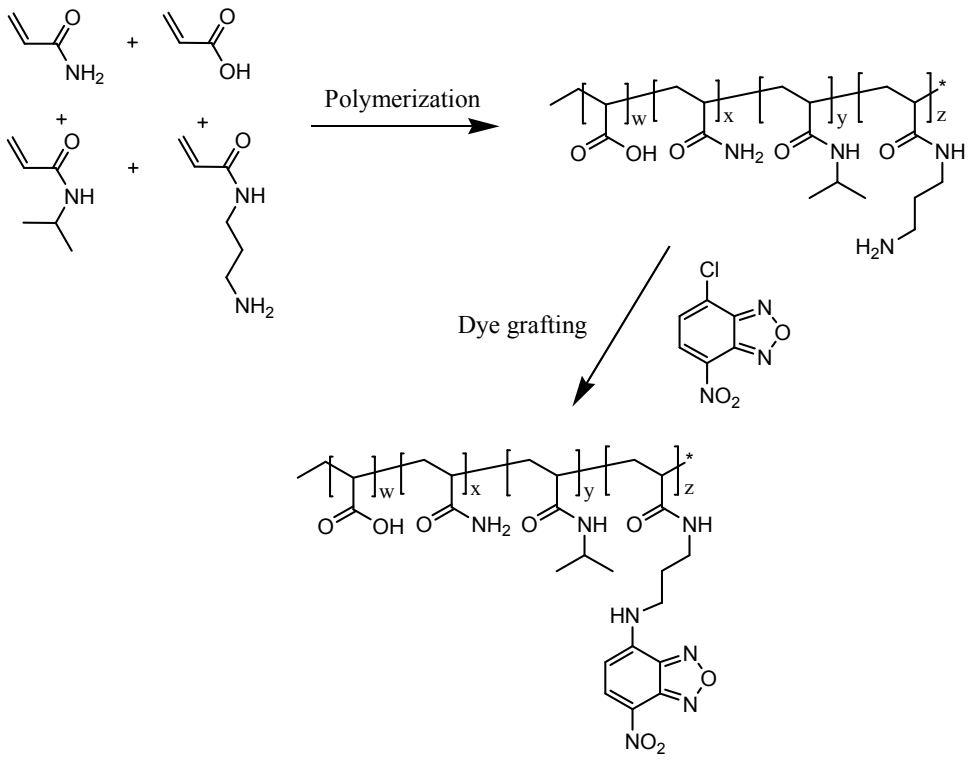

Figure 8: Schematic representation of preparation of NBD labeled NIP and MIPs. Cross linker, initiator, and porogen were omitted from the scheme for clarity (please see the text for detailed synthetic details).

The thoroughly washed and soaked NIP and MIP films were first cut into pieces of suitable size for inserting into the plastic cuvettes followed by dipping in the methanolic solution of NBD-Cl (0.020 g in 15 mL methanol) for 5 hours. To facilitate the reaction between the surface amine and NBD-Cl, 0.100 g of sodium hydroxide was added to the reaction mixture. After 5 hours of waiting, the dipped films now show intense yellow color that is due to the grafted NBD derivative on the polymer film. Thus obtained yellow polymer films were washed with large amounts of methanol to remove the excessive dye. Subsequently, the films were washed with copious amount of water and stored in water until use.

2.6. Preparation of fluorescence metal ion sensors

2.6.1. NBD-SG

NBD-SG was prepared using the following procedure (Figure 9). Compounds glutathione reduced (0.154 g, 0.5 mmol) and NBD-Cl (0.100 g, 0.5 mmol) were

dissolved in 10 ml water-methanol (v/v 1:1) mixture in a 50 mL round bottomed flask. The reaction mixture was stirred at room temperature for overnight. The yellow solid product was precipitated during the reaction. Thus obtained product was filtered and washed with water-methanol (v/v 1:1) mixture. The overall yield of the reaction is about 80%.

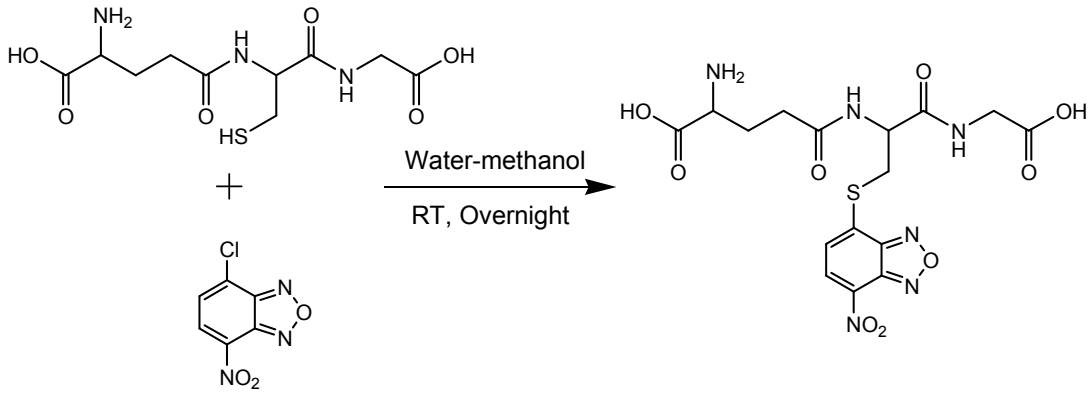

Figure 9: Preparation of NBD-SG.

2.6.2. NPS-SG

Compounds NPM (0.050 g, 0.168 mmol) and glutathione reduced (0.052 g, 0.168 mmol) were dissolved in a mixture with 1 ml of DMSO and 5 ml of water in a 50 mL round bottomed flask and was stirred at room temperature for overnight. Once again light yellow product of NPS-SG is precipitated out during the reaction. The solid product was washed with DMSO-water mixture (v/v, 1:5) and dried under reduced pressure. The overall yield of the reaction is 75%. The reaction scheme is shown in Figure 10.

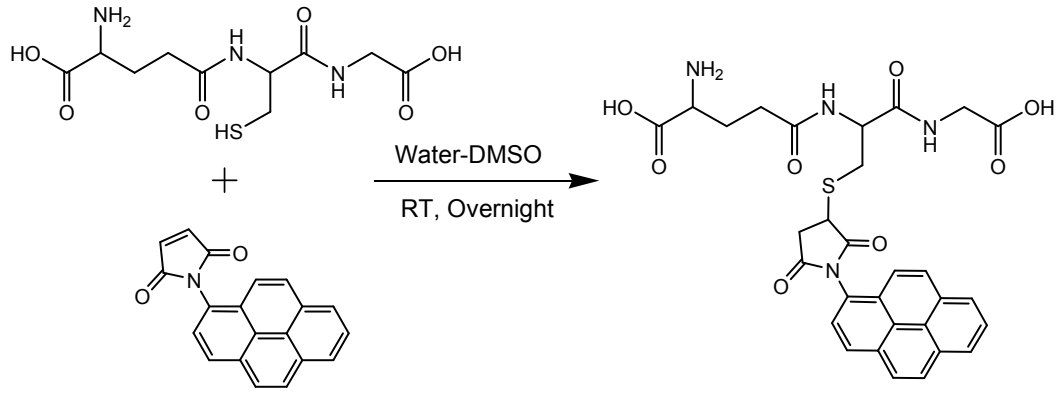

Figure 10: Preparation of NPS-SG.

2.7.Absorption and Fluorescence Spectroscopy

Absorption and fluorescence measurements were performed using Agilent UV-Visible diode-array absorption spectrophotometer or Molecular Devices spectrophotometer and Varian Cary Eclipse fluorescence spectrophotometer, respectively. Absorption measurements of the gold nanoparticles embedded films were conducted with a piece of the polymer placed in a 24-well plate and the film was held with black rubber 'O' ring. The fluorescence study of all other MIPs and NIPs with milk-filter membrane backing was obtained by using the regular cuvette holder equipped with a temperature controllable thermocouple connected to a Peltier cooling system is used for all fluorescence measurements. To facilitate insertion of the sensor into 3mL fluorescence plastic (polystyrene) cuvettes for reproducible analysis, the NIP and MIP films were cut into 1.1 x 2.5 cm pieces. These membrane backed stiff films are positioned diagonally in to the cuvette in the appropriate medium for all fluorescence measurements in water. The emission light is collected from the back of the film while illuminating from the front. The excitation spectra were collected at the fixed emission wavelength of 340 nm and slit-widths of 5 nm. All experiments were carried at room temperature (25 ± 2 °C). Time-resolved intensity decays were recorded using an ISS Koala fluorescence lifetime spectrometer. The excitation at ~ 370 nm was obtained using a LED.

Image analysis: Color changes of the imprinted and non-imprinted polymers were photographed using regular digital camera while the films were exposed to room light. The concentrations of the analytes were changed from 0 to 50 mM. The Photographs were taken after the films were incubated in the solutions of known concentration of analyte for 1 hr. The primary colors of the images were quantified using CorelDraw image analysis software with 24 bit (3X8) resolution. An average of over 50000 pixels was considered for the image analysis.

Data Analysis: The fluorescence intensity decays were analyzed in terms of the multi-exponential model as the sum of individual single exponential decays [56]:

$$I(t) = \sum_{i=1}^{n} \alpha_i \exp(-t/\tau_i) \qquad (1)$$

In this expression τ_i are the decay times and α_i are the amplitudes and $\sum_i \alpha_i$ = 1.0. The fractional contribution of each component to the steady-state intensity is described by:

$$f_i = \frac{\alpha_i \tau_i}{\sum_j \alpha_j \tau_j} \quad (2)$$

The average lifetime is represented by:

$$\bar{\tau} = \sum_i f_i \tau_i \quad (3)$$

The values of α_i and τ_i were determined using the ISS K2 Multifrequency phase fluorometer software with the deconvolution of instrument response function and nonlinear least squares fitting. The goodness-of-fit was determined by the χ^2 value.

3. Results and discussion

3.1. Molecular imprinted polymers

We successfully have developed several combinations of molecularly imprinted and non-imprinted polymers for three different and selected analytes, namely glutathione, caffeine and adrenaline. We used two kinds of probes as signal transducers that expected to probe the binding events of MIPs with analytes. They are plasmonic probes (gold nanoparticles) and organic probes based pyrene (NPM) and (nitrobenz-oxa-diazole (NBD). We first describe the results obtained from the MIPs and NIPs embedded with gold nanoparticles and subsequently we elaborate the corresponding data produced from NPM and NBD derivatized MIPs and NIPs.

3.1.1. MIPs and NIPs embedded with Gold nanoparticles

3.1.1.1. Plasmon absorption spectra of gold nanoparticles

We first measured the plasmon absorption spectra of produced gold nanoparticles in aqueous solution and compared it with the spectra from the particles within the polymer environment to understand the polymer effect on the plasmon absorption. Figure 11 shows the normalized plasmon absorption spectra of gold nanoparticles in water and embedded in polymer film. It also shows the absorption spectrum of blank polymer (blue line), that has no embedded gold nanoparticles. Blank polymer shows insignificant absorption contribution in the spectral region of interest. As can be seen from the figure, gold particles in water and in polymer exhibited very similar plasmon absorption spectral features, except an increase in the bandwidth in polymer. The increase in the bandwidth from the nanoparticle embedded polymer might due to (1) change in the gold particle size distribution during the polymerization process and/or (2) occurrence of expected inter-particle interactions between closely packed gold nanoparticles in the polymer. However, the observed data indicate these interactions or increase in particle size are minimum. If the increased bandwidth is solely accounted for the expected increased inter-particle interaction in polymer, the observed small changes might indicate insufficient particle density in the polymer. It is reported in the literature that the inter-particle interactions are dominant when the distances between the particles are well below 2.5 times the particle size [30].

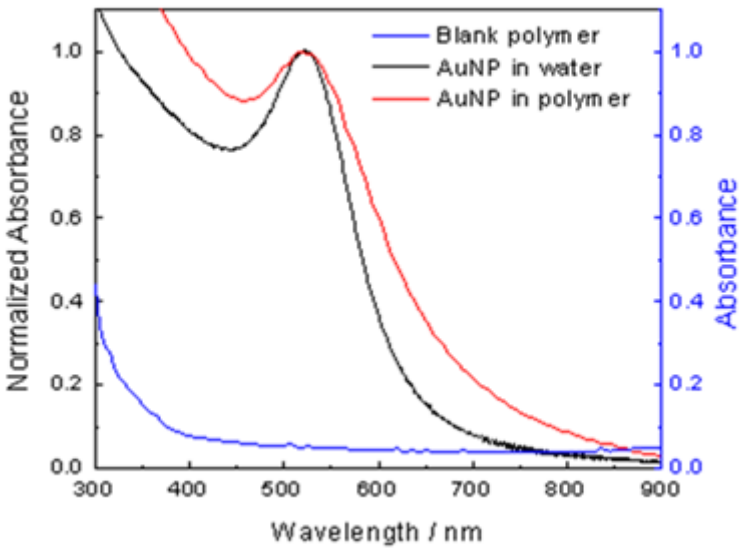

Figure 11: Normalized plasmon absorption spectra of as prepared gold nanoparticles (AuNP) in water and embedded in polymer. The absorption spectra of the blank polymer is also shown in the figure.

Considering the sizes of the particles (of ~ 10 nm) used in the present study, sufficient interparticle interactions are expected when the separating distances are below 25 nm. Figure 11 suggests that the inter-particle distances in the polymer are varied (wider bandwidth) but generally greater than 25 nm apart (too far apart for plasmonic interactions) and may be comparable to the distances in solution. As an alternative, using particles sized larger than those in the present study can increase the interparticle interactions while remaining at similar particle concentrations. However, it is worth noting that the polymer environment and polymerization procedure has minimum effect on the particle stability.

3.1.1.2. NIPs and MIPs response to analytes

Absorption spectroscopy: Figure 12 shows tail-matched (at 900 nm) plasmon absorption spectra of imprinted and non-imprinted polymers with 0 an 50 mM of caffeine. For these polymer films, both NIP and MIP, the plasmon absorption spectra of the gold nanoparticles have little response to caffeine. However, while the non-imprinted polymer (NIP) in water with caffeine shows almost no change in its spectra,

the corresponding molecular imprinted polymer is red-shifted by about 10 nm in the presence of 50 mM caffeine [Figure 12 (B)].

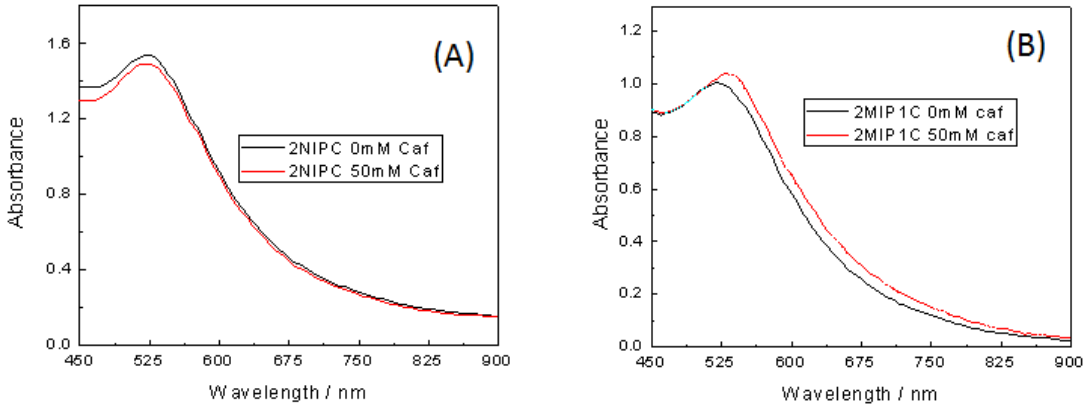

Figure 12: Tail-matched plasmon adsorption spectra of gold nanoparticles embedded in non-imprinted (A) and molecularly imprinted polymer (B) in water with 0 and 50 mM caffeine.

A very similar absorption spectral changes were noticed from the corresponding glutathione and adrenaline imprinted and non-imprinted polymers in water with in the presence of respective analytes. The measured spectra of the NIPs and MIPs within the presence of glutathione and adrenaline are shown in appendix. The observed red-shift is contrary to the design principle (Figure 3), where the analyte binding with the MIPs should cause the blue-shift. We have no explanation at this time, but we speculate that the high concentration (50 mM) of analyte used in the present study might induced the polymer shrinking (*vide infra*). Moreover, the observed small changes indicate that the added analyte has minimum or no effect on the extent of inter-particle interactions. This is not surprising to us considering the plasmon absorption spectra of gold particles embedded in the polymer (Figure 11). We currently are considering to optimize the conditions to prepare suitable polymers that show reasonably good response to the target analytes.

Image analysis: Figure 13 shows the photographs of the polymer films. The imprinted and non-imprinted polymers were photographed from the 90° angle to the surface normal using a regular digital camera while the films were exposed to room light. The concentrations of the analytes were changed from 0 to 50 mM. The Photographs were taken after the films were incubated in the solutions of known

concentration of analyte for 1 hr. Although, we noticed minute changes in the absorption spectra of the polymers, we observed significant color changes of the polymer films in the presence of analytes. Additionally, as can be seen from the photographs, the film physical dimensions were significantly reduced. This somewhat explains the observed red-shift in the absorption spectra of the MIPs in the presence of analyte (Figure 12). Further, to estimate the analyte induced color changes, we quantified the color contrast of the images (photographs) using CorelDraw image analysis software with 24 bit (3X8) resolution. An average of over 50000 pixels was considered for the image analysis. The obtained intensities of three primary colors decreased in the presence of caffeine. Figure 13 (B) shows a representative RGB intensity plot obtained for NIP and MIP with two different concentrations of caffeine. As can be seen from the figure the extent of color change is small with NIP as compared with that of MIP and it is well reflected in intensity change in the primary colors of the images shown in the right panel of the figure. Once again, we saw very similar response from the corresponding glutathione and adrenaline imprinted and non-imprinted polymers in the presence of respective analytes (please see the Appendix – AFigs. 2 and 4).

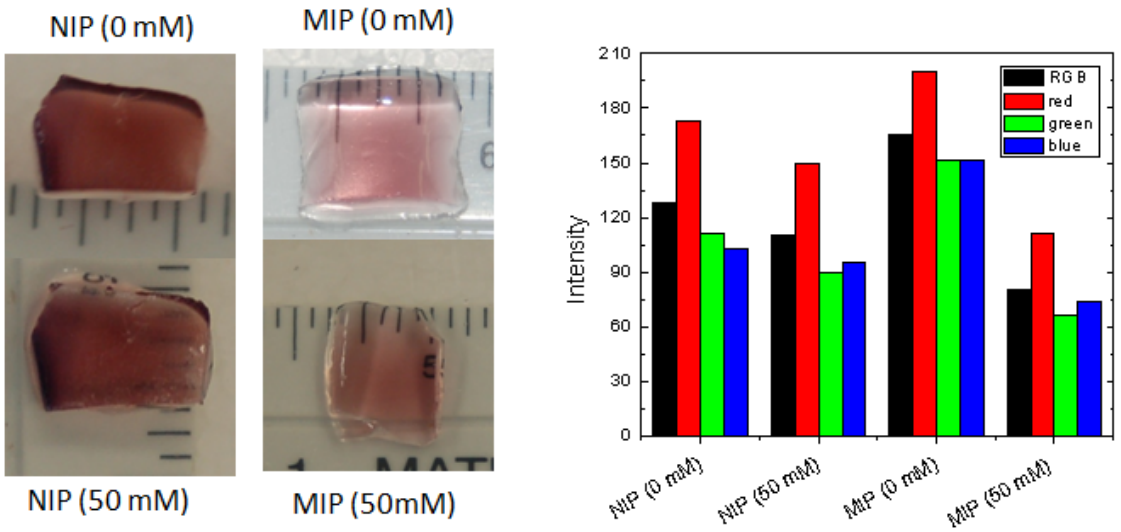

Figure 13: Photographs of non-imprinted polymer (NIP) and molecular imprinted polymers (MIP) with 0 and 50 mM caffeine (Left). Right side panel shows the corresponding intensities of primary colors with respect to caffeine concentrations obtained from the photographs shown in the left panel.

This study corroborates that the quantification of primary colors indeed provide information regarding analyte concentration in the sample. However, as from the strategy of the present study, the presence of analyte should increase the inter-particle distance in the polymer and accordingly one should anticipate the fade in polymer color. The observed contrasting color change is somewhat understandable when the physical shape (size) of the polymer is considered. For example, as mentiond previously, the dimensions of the polymer film (especially MIP) were reduced drastically within the presence of the 50 mM analyte. This unforseen shrinking of the polymer (especially MIPs) in the presence of analytes might be due to large excess of used analyte concentrations that might induce modulations in overall polymer morphology. In principle, the analyte binding should induce the swelling of the MIPs. To understand this in more detail, we further quantified the images of the polymers with lower concentrations of analytes and with more concentration intervals. Accordingly, thus obtained intensity changes with respect to analyte concentration were shown in Figure 14. As can be seen from the figure the intensities of the primary colors were systematically increased with increasing with the analyte concentrations up to about 10 mM. After that the polymer started shrinking and the intensities were dropped as it was observed in Figures 13. This indicates that the NIPs and MIPs are simply bind to the analytes without undergoing any change in polymer morphology in low ananlyte concentration range of up to 10 mM.

To compare the response of NIP and corresponding MIP with the analyte we normalized the intensities of the primary colors. Figure 15 shows the normalized intensities obtained for 2NIP and 2MIP1 (caffeine imprinted) and 2NIP and 2MIP3 (glutathione imprinted) with caffeine and glutathione, respectively. As it can be seen from the figure, NIP shows almost very similar response to both the analytes studied. However, MIP1 response to caffeine is somewhat better than that of the MIP3 response to glutathione. Actually, this is not a fair comparison. But somehow the MIP3 response to glutathione is different. We are currently considering further experiments to understand this ambiguity.

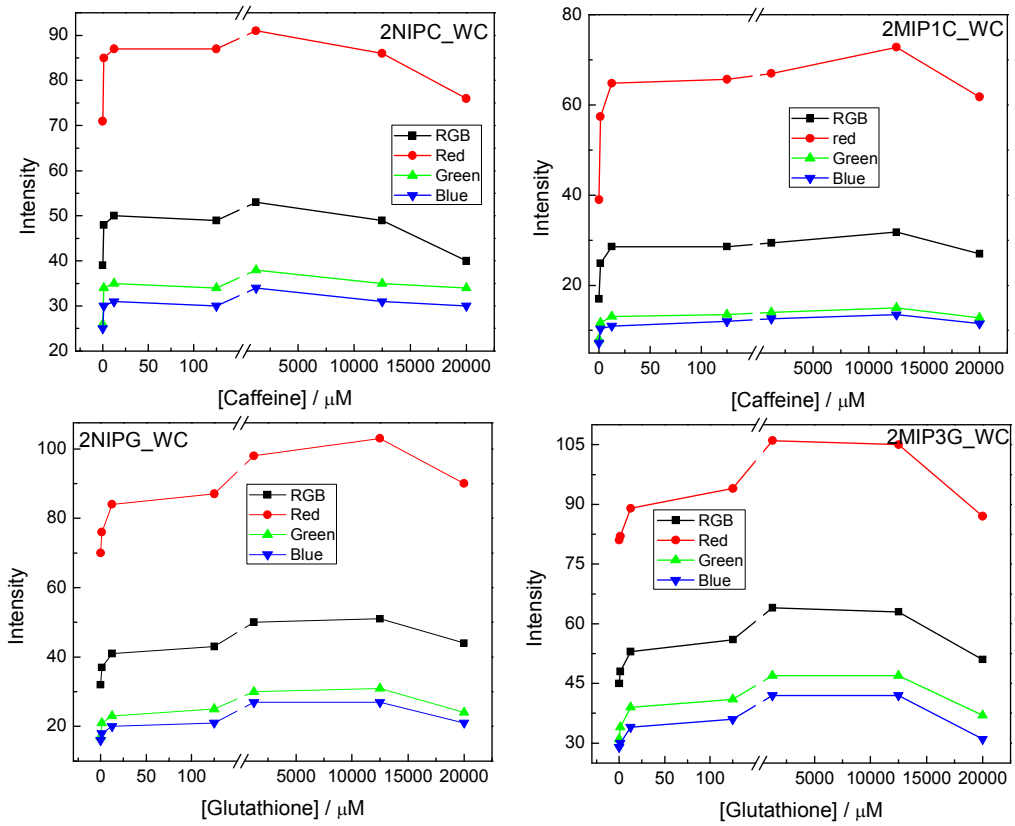

Figure 14: Intensities of RGB and three primary colors estimated from the photographs of NIPs (Left) and MIPs (Right) with caffeine (top) and glutathione (bottom) respectively.

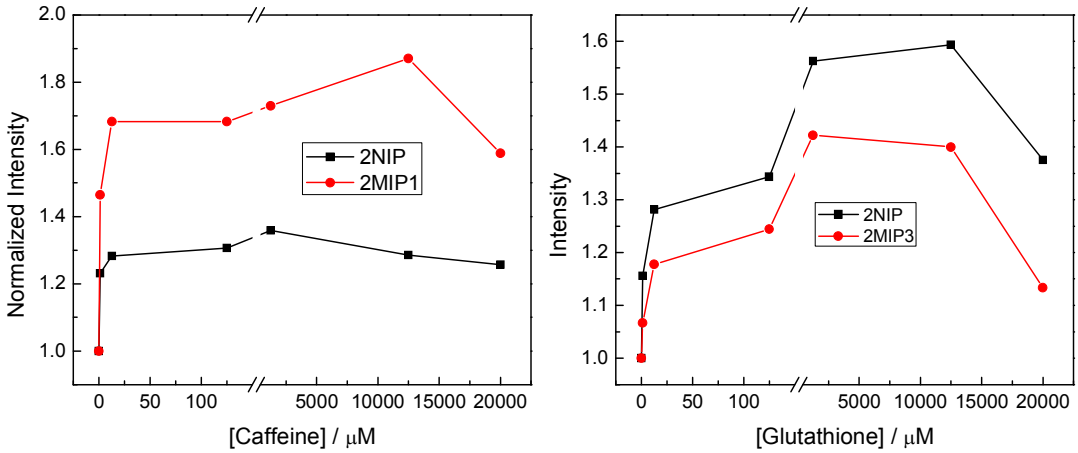

Figure 15: Normalized RGB estimated for 2NIP and 2MIP1 (left) and 2NIP and 2MIP3 with caffeine and glutathione, respectively (the other three primary colors were omitted for clarity).

3.1.2. NPM labeled MIPs and NIPs

As previously stated, part of our efforts is to explore the fluorophores as alternative signal transducers to the nanoparticles. Thus, we focused our interest on the optimization of the NPM labeled poly(N-isopropyl)acrylamide gels as potential MIPs. In general, pyrene derivatives such as NPM when in close proximity form dimers in the excited state and, thus, emit a distinct excimer fluorescence emission. Because, this phenomenon is proximity-dependent it is primarily affected by the pyrene concentration. Subsequently, we anticipate that altering the local concentration of the immobilized pyrene derivative (NPM) in the imprinted polymer as the analyte binds to the MIP can change the monomer-excimer intensity ratio. This is indeed very similar to the inter-particle distance dependent plasmon absorption properties of gold nanoparticles discussed in the last paragraphs. Considering this and to optimize the polymer composition and probe concentration suitable for imprinting applications, we initially prepared non-imprinted polymer consisting of known concentrations of NPM. The polymer preparation and subsequent treatment is described in experimental section.

3.1.2.1. Temperature response

To test the suitability of the obtained film we measured its temperature response. This is because poly(N-isopropyl)acrylamide gels are known to show abrupt changes in polymer morphology (i.e. polymer swelling) with temperature with a lower critical solution temperatures (LCST) in near biological temperature. This study will eventually be useful in optimizing the polymerization conditions and probe concentrations to obtain maximum spectral changes during analyte binding with the MIPs.

Figure 16 shows the fluorescence emission spectra of NPM labeled polymer film in water at various temperatures. The NPM film was placed diagonally in 3 mL water containing cuvette with front-face illumination. To minimize the scattering from the sample, the emission was collected from the rare-side of the film. The cuvette holder is equipped with a thermocouple, temperature controller and a water circulation pump. The emission spectra were collected at 10 to 70 °C with 5° C intervals. As can be seen from the figure, NPM labeled polymer showed emission largely from the monomer with band maximum at 420 nm. Although, it is not visible from the figure corresponding excimer emission can be seen at about ~480 nm. A more distinguishable emission from

the excimer can be obtained when the higher concentration of NPM is used during the polymer preparation. Nevertheless, we observed a systematic increase and decrease in monomer and excimer emission intensities (respectively) with increasing temperature. These observed spectral changes can be attributed to increase in the separation distance between two neighboring pyrene moieties due to temperature induced swelling of the polymer films. Figure 16 (B) shows corresponding ratiometric response curve plotted against the sample temperature. A similar situation can be expected when the MIPs developed with NPM bind with the target analyte.

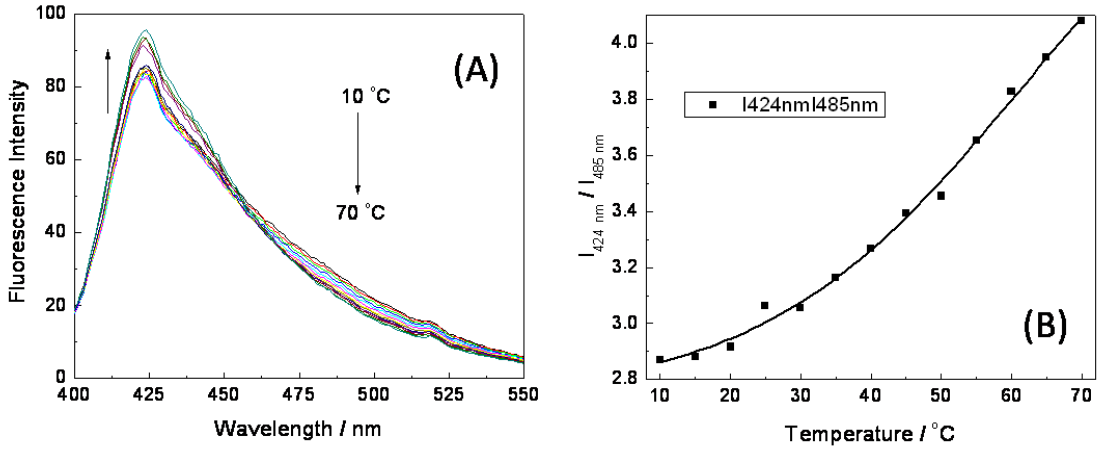

Figure 16: (A) Fluorescence emission spectra of NPM immobilized non-imprinted polymer immersed in water, λex = 380 nm. Panel (B) shows the corresponding emission wavelength response to temperature of the medium.

3.1.2.2. NPM labeled NIPs and MIPs response to analytes

Anticipating the better results with the NPM derivatized films over gold nanoparticles embedded ones, we prepared NPM co-immobilized non-imprinted and imprinted polymers with two different analytes, caffeine and glutathione. To maximize the excimer emission we used double the amount of NPM (40 mg/3mL). As described in the experimental section, the NIP and MIP1 (caffeine imprinted) and MIP3 (glutathione imprinted) were prepared from the prepolymer mixture of *N*-isopropylacrylamide, acrylic acid in DMSO at 70° C. AIBN was used to initiate the reaction and *N*,*N*'-methylenebisacrylamide is used as the cross linker.

Figure 17 shows the fluorescence emission spectra of NPM labeled NIP within the presence of varied concentrations of glutathione. As the result of using high concentration of dye, we have noticed prominent broad and structure-less emission at about 470 nm from its excimer. Corresponding structured monomer emission (that is actually almost buried underneath the excimer emission) at about 405 nm is not clearly resolved. Figure 17 shows the fluorescence emission spectra of NPM labeled MIP with increasing concentration of caffeine. As can be seen from the figure, we noticed a systematic decrease and increase in excimer and monomer intensity, respectively, with increasing concentrations of caffeine. Also shown in the figure is the ratiometric response of the NIP and MIP with increasing concentration of caffeine. It is clear from the figure that the response of both NIP and MIP is almost similar. A similar response is also noticed with the glutathione imprinted and non-imprinted polymer in the presence of glutathione (see AFig. 5 of Appendix). This observed weak response from MIPs might ascribe to the difference in the polarity of the solvents used for the polymer fabrication and analysis study. Considering the solubility of the probe NPM, DMSO was used as porogenic solvent, whereas aqueous medium was used for analysis. These drastic changes in the solvent polarity might destroy the fabricated molecular imprinted cavities and hence MIPs are no longer selective for their respective analytes. Thus the observed spectral changes are might due to the non-specific bindings of analytes to the labeled polymer. We further considering to make the NIP and MIPs in aqueous solvent to preserve the produced molecular imprinted cavities.

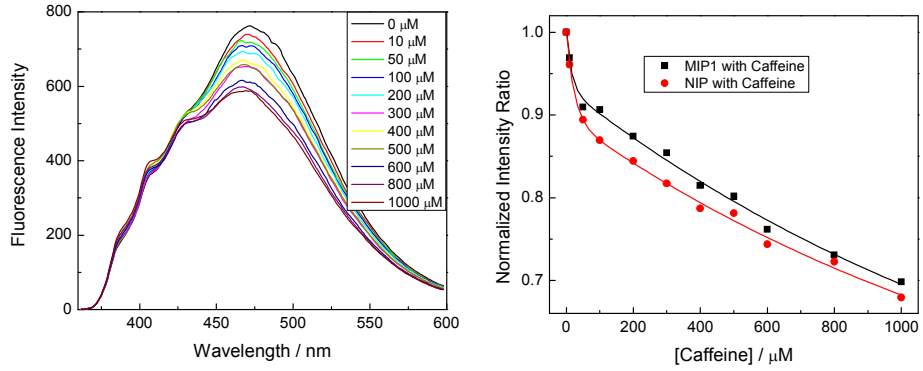

Figure 17: Fluorescence emission spectra of NPM immobilized and caffeine imprinted polymer in water with increasing concentrations of caffeine (left). The right panel shows the intensity ratio of NPM labeled NIP and MIP plotted against the caffeine concentration (λex = 340 nm).

3.1.3. NBD labeled MIPs and NIPs

Attempts to fabricate the NPM labeled NIP and MIPs in water were unsuccessful. This is largely because of the poor solubility of NPM in water. To avoid this, an approach of post-grafting (post-doping) the dye on to the blank polymer is applied. Accordingly, as described in the experimental section (section 2.5.3), the blank polymer of NIP and MIP (imprinted with water soluble glutathione) were fabricated first. Subsequently the dye 4-amino-7-nitrobenz-oxa-diazole was immobilized onto the polymer surface using methanolic NBD-Cl. Similarly, NPM can also be post-grafted on to the polymer when the polymer consist free thiol groups on its surface. The free thiol groups on the surface can be obtained when *N,N'*-bis(acrylolyl)cystamine is used instead of *N*-(3-aminopropyl)methacrylamide in the copolymerization.

Response of NBD labeled NIP and MIP: Figure 18 shows the fluorescence emission spectra of NBD labeled MIP in water with increasing concentrations of glutathione. As it can be seen from the figure, MIP shows typical broad emission spectrum that is attributable for 4-amino-7-nitrobenz-oxa-diazole. The fluorescence intensity of the system is increased with increasing the glutathione concentration. Along with the increase in intensity, it is also clear from the figure that, MIP shows slight blue-shift in its emission spectrum. This indicates that the MIP binding with the glutathione decreases the local polarity of the polymer. NBD derivatives are commonly used as polarity sensitive probes. Emission spectrum from the corresponding NIP shows very minute increase with increasing concentration of the glutathione. This is indeed very clear from the Figure 18 (right) where the normalized intensities of MIP and NIP are plotted against the glutathione concentration.

Selectivity of NBD labeled MIP to glutathione: Although, we have better response from the MIP over NIP, the observed net change is only about 15%. However, it is interesting to note that the selectivity of the NBD labeled MIP, that is molecularly imprinted using the template SSG, shows systematic differentiations in its response to several structurally similar compounds. For example, the selectivity of the MIP was tested with SSG, glutathione (reduced), glutathione (oxidized) and caffeine. Figure 19 shows the normalized intensities of MIP in water with several analytes. As it can be seen from the figure, NBD labeled MIP shows high selectivity to SSG (that is used as template while making the MIP) over glutathione (reduced) and it is further reduced for

glutathione (oxidized). Additionally, the MIP response to structurally very different caffeine is negligible. This is indeed one of the interesting and important results of our findings so far.

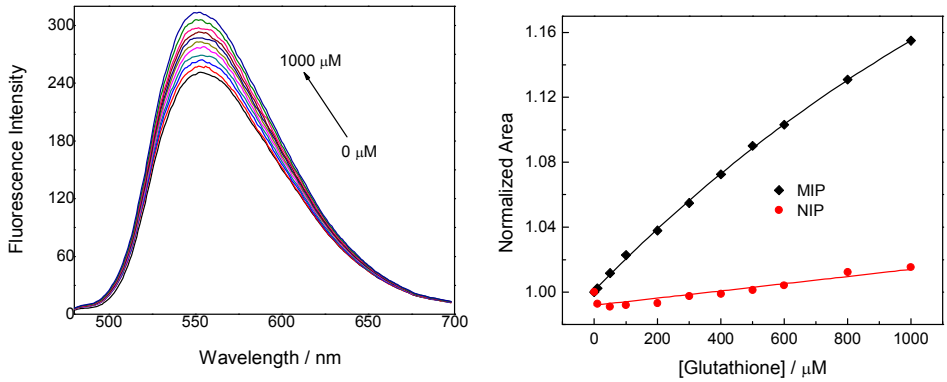

Figure 18: Fluorescence emission spectra of NBD labeled MIP in water with increasing concentrations of glutathione (left) (λex = 450 nm). Right panel shows the normalized intensity of MIP and NIP response to glutathione.

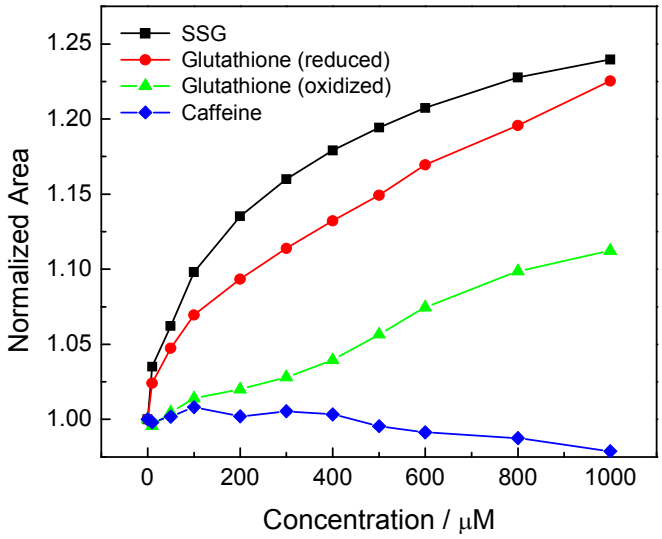

Figure 19: NBD labeled MIP response to different analytes.

3.2. Fluorescence metal ion sensors synthesis and reponse

Design and development of novel fluorescence sensors are an important aspect of current research. Here we used small oligopeptide, glutathione, as the ion recognition moiety for the first time. Glutathione is a tripeptide and thus have multi-full functional

groups that can bind with metal ions. Additionally, it has a free sulfidral group and expected to bind with soft metal ions as well. Considering this, we prepared two fluorescence sensors, NBD-SG and NPS-SG. First we describe the metal sensing behavior of the NBD-SG followed by NPS-SG.

3.2.1. NBD-SG

As described in the experimental section, NBD-SG has been produced in large quantity. It is fairly soluble in water and show absorption and emission band maximum at 420 and 520 nm respectively. Both absorption and emission spectra are broad and structureless. After having preliminary investigations on the photophysical behavior of NBD-SG, we tested for its metal sensing behavior in water. Figure 20 shows the fluorescence emission spectra of NBD-SG in water with increasing concentrations of toxic mercuric ion (Hg^{2+}). As can be seen from the figure, the fluorescence intensity of the NBD-SG is decreased with increasing concentration of Hg^{2+}. Additionally, it is also noted from the figure that the emission spectra shows red-sift. We are yet to have clear explanation for the observed spectral changes. However, the observed shift and intensity drop can be ascribed to the mercuric ion induced stabilization of intermolecular charge transfer (ICT) of NBD derivatives.

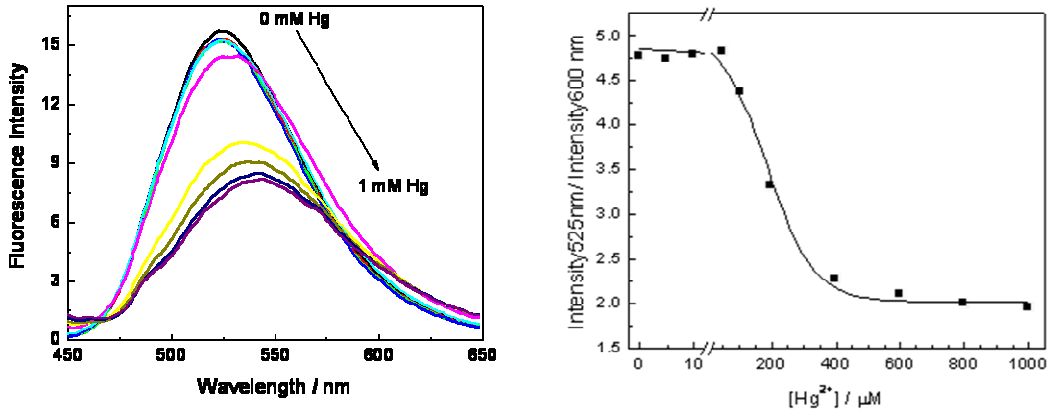

Figure 20: Fluorescence emission spectra of NBD-SG in water with Hg^{2+} (λex = 420 nm). Right panel shows the ratiometric response of NBD-SG to Hg^{2+}.

To test the suitability of the probe to other metal ions, we measured the absorption and fluorescence spectra of NBD-SG in water with in the presence different concentrations of 18 more metal ions from all over the periodic table. Interestingly, NBD-SG shows no response to any other metal ion studied. This can be evidenced by the Figure 21. The silence nature of the probe to any other metal might be due to inadequate effect of the bound metal ions on the electronic configuration of the probe NBD. This can be feasible when the metal ions are bound with only peripheral functional moieties and not engaging with the thiol group that is directly attached to the NBD ring. On the other hand, because of soft nature of Hg^{2+} such an interaction with thiol can be expected. Accordingly, NBD-SG seems selective for Hg^{2+} among several other metal ions studied. A detailed investigation is underway to understand the plausible binding and sensing mechanism.

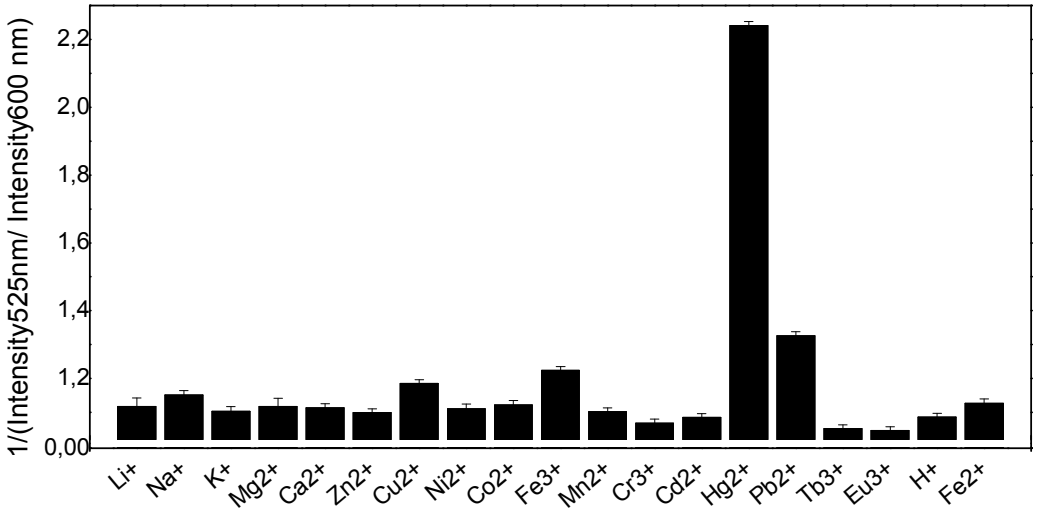

Figure 21: NBD-SG response to various metal ions.

3.2.2. NPS-SG

To further understand and to generalize the selectivity criteria of the NBD-SG to Hg^{2+}, we prepared NPS-SG. Here in the case of NPS-SG, thiol group of glutathione is remotely connected to the probe. This eliminates the feasibility of modulating the electronic configurations of the probe under investigation. However, many aromatic compounds including pyrene show photoinduced inter/intermolecular electron transfer (PET) properties when the electron donor/acceptor group is suitable positioned. In NPS-

SG, one can anticipate such interactions might be feasible from the appending carboxylic groups and/or amine moiety of glutathione. A detailed investigation is under consideration to understand this phenomenon.

NPS-SG is produced in single step reaction from the previously synthesized NPM. The synthetic details are depicted in experimental section. Once again NPS-SG is fairy soluble in water. Subsequently, we tested for the metal ion sensing ability of the probe in water. Figure 22 shows the fluorescence excitation spectra of NPS-SG in water with Cr^{3+}, Fe^{3+} and Hg^{2+}. Unlike NBD-SG, NPS-SG shows response towards a few metal ions. This is more clear from the Figure 23. This indicates the feasible binding ability of glutathione moiety with several metal ions. These binding events were not visualized while using NBD-SG. A similar response is also noticed from the lifetime based measurements. Further investigations are under consideration.

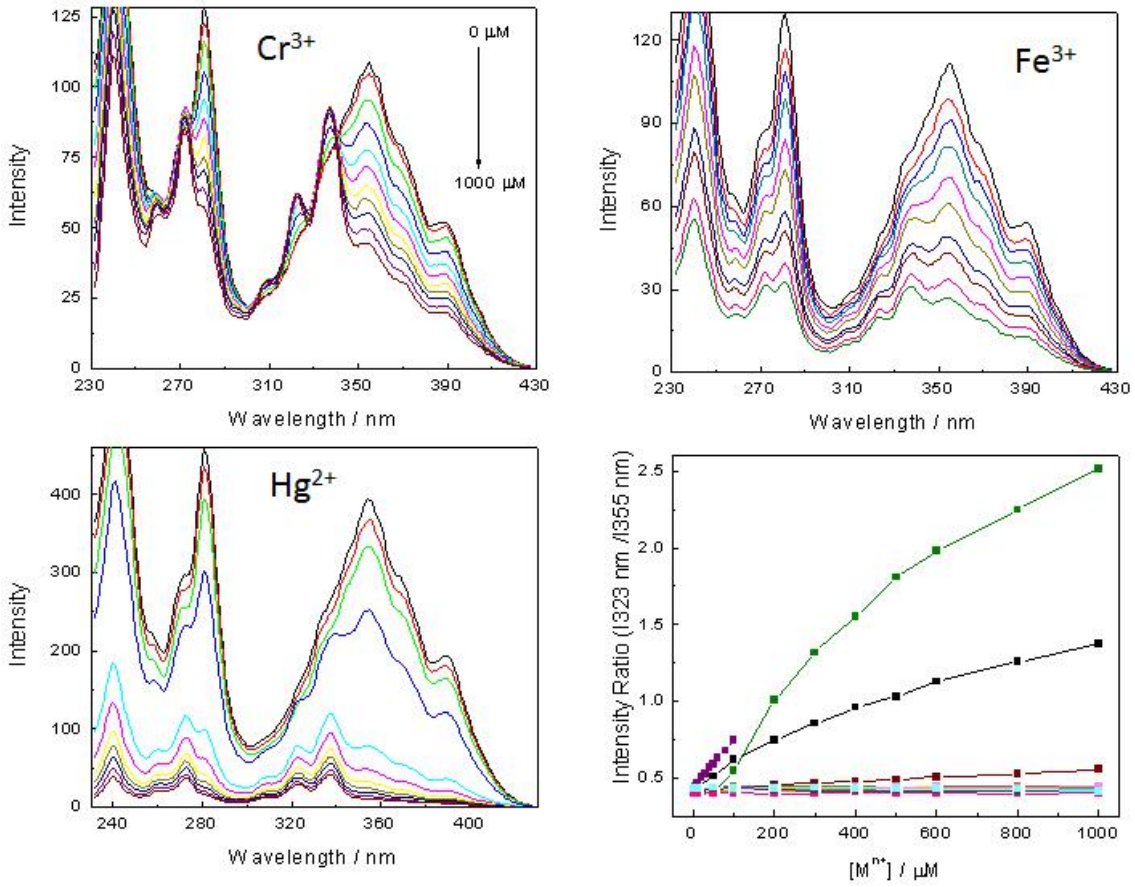

Figure 22: Fluorescence excitation spectra of NPS-SG in water with Cr^{3+} (top left), Fe^{3+} (top right) and Hg^{2+} (bottom right) (λem = 450 nm). The right bottom shows the corresponding ratiometric plot of NPS-SG in water with 19 different metal ions.

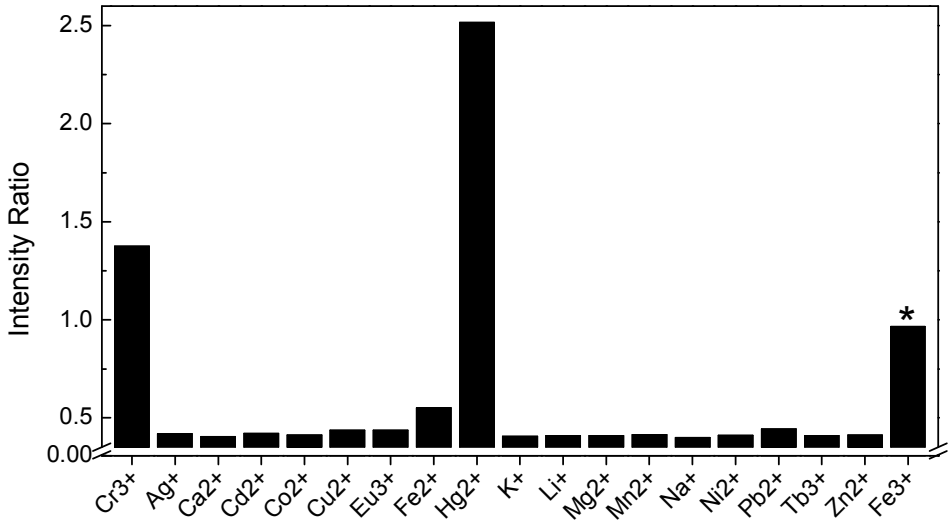

Figure 23: NPS-SG response to various metal ions in water. * Fe^{3+} concentration is 100 μM, where as the concentration of other metal ions are 1 mM.

4. Conclusions

In this thesis we presented our preliminary efforts in the development of molecularly imprinted polymers (MIPs) specifically for three small-molecule biomarkers, including glutathione, caffeine and adrenaline. We took two different approaches. In the first approach, we employed gold nanoparticles as the signal transducers whereas the second approach utilized organic fluorophores as optical signaling units for the events associated with analyte binding to MIPs. The molecularly imprinted polymers embedded with gold nanoparticles showed systematic changes in their absorption spectra with increasing concentrations of target analytes and exhibited color changes distinguishable by the naked eye. Subsequently, the intensity contributions of three primary colors (RGB) of the images of MIPs were estimated. It is clear from our initial findings that the nanoparticle size has to be increased in order to observe proximity dependent plasmonic interactions. Additionally, the film has to be made more robust and uniform in thickness.

We have shown that this can be done while using organic probes such as NPM and NBD, where the sensing polymer film reported here was polymerized between two glass plates and supported with a filter paper backing. Preliminary imprinting studies using NPM as the signaling probe showed minimal response. Especially, unforeseen loss of MIPs selectivity is noticed. This is attributed to the variations in the polarity of the solvent used for the preparation and analysis. To circumvent this we end up with using an approach of post-grafting of the dye. This method involves the synthesis of the blank NIP and MIP and subsequent tethering of the fluorescent dye to the surface appending reactive functional groups. Accordingly, we successfully tethered NBD moieties to the polymer. NBD labeled NIP and MIP show systematic response and high selectivity to the template molecule SSG.

The second part of the thesis describes the synthesis and metal ion sensing ability of two newly developed molecules, NBD-SG and NPS-SG. NBD-SG shows selective response to mercuric ion. On the other hand NPS-SG has shown response to a few metal ions including Fe^{3+}.

5. Evaluation of work conducted

The work presented in the thesis provides significant breakthrough for the development of the sensor systems using molecular imprinted polymers with much improved sensitivity and selectivity. With this work our group at CAST adventured into a new field of science that can provide enormous opportunities to construct new generation of sensors of interest. We are expecting that the present work provides sufficient basic knowledge for further advancement within this project.

5.1. Accomplished objectives

The data presented in this thesis has accomplished several objectives. The first objective of this project is that the understanding of the suitable conditions, polymer composition, choice of probe, probe concentrations for appropriate imprinting. We evaluated the suitability of several probes, conditions and so on. We noticed interesting results with gold nanoparticles and with all three analytes we studied in the short period of time, the optimization of several more conditions will result suitable materials for efficient sensing applications. The second objective of the project is to test the suitability of the organic fluorescent probes that provide additional spectroscopic methods apart from absorption spectroscopy. We succeeded this object with using NPM and NBD. Additionally, we developed two new metal ion sensors, one of which is selective for mercuric ion.

5.2. Limitations and future work

Primary limitation of this project is time. We have very little time. Additionally, molecular imprinting is somewhat time consuming and tedious process. It involves with several iterations to have the suitable sensing material. Additionally, sometimes we noticed probes instability during the polymerization process. Otherwise, molecular imprinting of polymers provides novel sensors for any analyte of interest.

As shown, the absorption spectral changes in response to binding of analyte to MIPs, especially shift in the plasmon absorption band, are very low. This is primarily because of little/no inter-particle interactions between the embedded gold nanoparticles in the polymer. The inter-particle interactions are dependent on both size and distance

between the interacting particles: the interaction becomes zero as the distances become greater than 2.5 times the particle size. Accordingly, we can improve the magnitude of the signal change by increasing the particle concentration or increasing the particle size. Increasing the concentration leads to films with very dark colors with very little light transmission. Thus, attempts to prepare large sized particles are in progress. Further, we will optimize the dynamic range of the MIPs especially glutathione sensitivities at near physiological requirements. This can be done by adjusting the template/analyte concentration during MIP fabrication. Additionally, the techniques employed in the pH sensing film to produce MIPs of uniform thickness and with backing support will be utilized in the MIP fabrication. The second set of sensing systems with NPM and especially NBD has resulted promising results. It indicates that post-grafting of the suitable dye might be an appropriate approach. Although, we have very interesting results from the newly developed fluorescence metal ion sensors, we need to perform systematic study to reveal the underling sensing modality. Also the compounds analysis is to be conducted before publishing the data. At least three manuscripts are in the process of being prepared for publication.

5.3. Final deliberation

The present project that is a part of my master degree has given me an opportunity to learn new techniques, to explore new culture and mingle with new friends in the foreign country. The project we did is amazing. It is a growing subject with high-end future. We had have chance to learn lot about fluorescence. We hope the molecular imprinting will be part of my curriculum of research.

6. References

1. Alexander, C.; Andersson, H.S.; Andersson, L.I.; Ansell, R.J.; Kirsch, N.; Nicholls, I.A.; O'Mahony, J,; Whitcombe, M.J. (2006). Molecular imprinting science and technology: a survey of the literature for the years up to and including 2003, *J. Mol. Recogni., 19 (2)*, 106-180.
2. Li, R. X.; Dowd, V.; Steward, D. J.; Burton, S. J.; Lowe, C. R. (1998). Design, synthesis, and application of a Protein A mimetic, *Nat. Biotechnol.*, *16*, 190-195.
3. Shea, K. J. (1994). Molecular imprinting of synthetic network polymers – the de-novo synthesis of macromolecular binding and catalytic sites, *Trends Polym. Sci.*, *2*, 166.
4. Wulff, G. (1995). Molecular imprinting in cross-linked materials with the aid of molecular templates – a way towards artificial antibodies, *Angew. Chem., Int. Ed. Engl.*, *34*, 1812.
5. Steinke, J.; Sherrington, D. C.; Dunkin, I. R. (1995). Imprinting of synthetic polymers using molecular templates, *Adv. Polym. Sci.*, *123*, 80.
6. Vidyasankar, S.; Ru, M.; Arnold, F.H.; (1997). Molecularly imprinted ligand-exchange adsorbents for the chiral separation of underivatized amino acids. *J. Chromatography A, 775 (1-2)*, 51-63.
7. Mosbach, K.; Ramstrom, O. (1996). The emerging technique of molecular imprinting and its future impact on biotechnology, *BioTechnology*, *14*, 163.
8. Sellergren, B. (1997). Noncovalent molecular imprinting: Antibody-like molecular recognition in polymeric network materials, *Trends Anal. Chem.*, *16*, 310-320.
9. Takeuchi, T.; Haginaka, J. (1999). Separation and sensing based on molecular recognition using molecularly imprinted polymers, *J. Chromatogr. B, 728*, 1-20.
10. Lehn, J-M. *Supramolecular Chemistry*; Wiley-VCH: Weinheim, 1995.
11. Vlatakis, G.; Andersson, L. I.; Muller, R.; Mosbach, K. (1993). Drug assay using antibody mimics made by molecular imprinting, *Nature*, *361*, 645.
12. Al-Kindy, S.; Badía, R.; Suárez-Rodríguez, J. L.; Díaz-García, M. E., (2000). Molecularly imprinted polymers and optical sensing applications. *Crit. Rev. Anal. Chem., 30*, 291–309.

13. Sellergren, B. (1994). Direct drug determination by selective sample enrichment on an imprinted polymer, *Anal. Chem., 66*, 1578.
14. Wulff, G.; Haarer, J. (1991). Enzyme-analog built polymers 29. the preparation of defined chiral cavities for the racemic-resolution of free sugars, *Makromol. Chem.*, *192*, 1329.
15. Fischer, L.; Muller, R.; Ekberg, B.; Mosbach, K. (1991). Direct enantioseparation of beta-adrenergic blockers using a chiral stationary phase prepared by molecular imprinting, *J. Am. Chem. Soc., 113*, 9358.
16. Sellergren, B.; Shea, K. J. (1993). Influence of polymer morphology on the ability of imprinted network polymers to resolve enantiomers, *J. Chromatogr.*, *635*, 31.
17. Kriz, D.; Berggren-Kriz, C.; Andersson, L. I.; Mosbach, K. (1994). Thin-layer chromatography based on the molecular imprinting technique, *Anal. Chem.*, *66*, 2636.
18. Alvarez-Lorenzo, C.; Concheiro, A. (2004). Molecularly imprinted polymers for drug delivery, *J. Chromatogr. B, 804*, 231-245.
19. Schweitz, L.; Anderson, L. I.; Nilsson, S. (1997). Capillary electrochromatography with predetermined selectivity obtained through molecular imprinting, *Anal. Chem.*, *69*, 1179.
20. Cormack, P. A. G.; Elorza, A. Z. (2004). Molecularly imprinted polymers: synthesis and characterization, *J. Chromatogr. B, 804*, 174.
21. Flory, P. J. *Principles of Polymer Chemistry*, Cornell University Press, 1953.
22. Haupt, K.; Mosbach, K. (2000). Molecularly imprinted polymers and their use in biomimetic sensors, *Chem. Rev., 100*, 2495-2504.
23. Ye, L.; Mosbach, K. (2002). Molecularly Imprinted Materials: Towards the Next Generation, *Mat. Res. Soc. Symp. Proc., 723*, M3.1.1-M3.1.9.
24. Ramström, O.; Ye, L.; Mosbach, K. (1998). Screening of a combinatorial steroid library using molecularly imprinted polymers, *Anal. Commun., 35*, 9.
25. Ditlbacher, H.; Felidj, N.; Krenn, J.R.; Lamprecht, B.; Leitner, A. (2001). Aussenegg, F.R., Electromagnetic interaction of fluorophores with designed two-dimensional silver nanoparticle arrays, *Appl. Phys. B., 73*, 373-377.

26. Otto, A.; Mrozek, I.; Grabhorn, H.; Akemann, W., (1992). Surface-enhanced raman-scattering, *J. Phys. Condensed Matter, 4 (5),* 1143-1212.
27. Kreibig, U.; Vollmer, M. Optical Properties of Metal clusters, Springer Series in Material Science, Val. 25, (Springer,Berlin), 1995.
28. Yguerabide, J.; Yguerabide, E. E., (1998). Light-scattering submicroscopic particles as highly fluorescent analogs and their use as tracer labels in clinical and biological applications – I. Theory, *Anal. Biochem., 262*, 137-156.
29. Yguerabide, J.; Yguerabide, E. E., (1998). Light-scattering submicroscopic particles as highly fluorescent analogs and their use as tracer labels in clinical and biological applications – II. Experimental characterization, *Anal. Biochem., 262*, 157-176.
30. Su, K.-H.; Wei, Q.-H.; Zhang, X.; Mock, J. J.; Smith, D. R.; Schultz, S. (2003). Interparticle coupling effects on plasmon resonances of nanogold particles, *Nano Lett., 3*, 1087.
31. Maya, K. S.; Patil, V.; Sastry, M. (1997). On the stability of carboxylic acid derivatized gold colloidal particles: The role of colloidal solution pH studied by optical absorption spectroscopy, *Langmuir*, *13*, 3944.
32. Reynolds, R. A.; Mirkin, C. A.; Letsinger, R. L. (2000). Homogeneous, nanoparticle-based quantitative colorimetric detection of oligonucleotides, *J. Am. Chem. Soc.*, *122*, 3795.
33. Mirkin, C. A.; Letsinger, R. L.; Mucic, R. L.; Storhoff, J. J., (1996). A DNA-based method for rationally assembling nanoparticles into macroscopic materials, *Nature, 382*, 607.
34. Kim, Y.J.; Johnson, R. C.; Hupp, J. T. (2001). Gold nanoparticle-based sensing of "spectroscopically silent" heavy metal ions, *Nano Lett., 1*, 165.
35. Lin, S. Y.; Liu, S. W.; Lin, C. M.; Chen, C. H. (2002). Recognition of potassium ion in water by 15-crown-5 functionalized gold nanoparticles, *Anal. Chem*., *74*, 330.
36. Thanh, N. T. K.; Rosenzweig, Z. (2002). Development of an aggregation-based immunoassay for anti-protein A using gold nanoparticles, *Anal. Chem.*, *74*, 1624.

37. Matsui, J.; Akamatsu, K.; Nishiguchi, S.; Miyoshi, D.; Nawafune, H.; Tamaki, K.; Sugimoto, N.; (2004). Composite of Au nanoparticles and molecularly imprinted polymer as a sensing material, *Anal. Chem., 76,* 1310-1315.
38. Mistry, P.; Harrap, K.; (1991). Historical aspects of glutathione and cancer chemotherapy, *Pharmacol Ther, 49,* 125.
39. Meister, A.; (1994). Gluthathione, ascorbate and cellular protection, *Cancer Res, 54 (Supplement 7)*, 1969-1975.
40. Voehringer, D.; JcConkey, D.; McDonnell, T.; Brisbay, S.; Meyn, R.; (1998). Bcl-2 expression causes redistribution of glutathione to the nucleus, *Proc. Nat. Acad. Sci., 95*, 2956-2960.
41. Lautier, D.; Canitrot, Y.; Deeley, R.; Cole, S.; (1996). Multidrud resistance mediated by the multidrug resistance protein (MRP) gene, *Biochem. Pharmacol., 52*, 967-977.
42. Shiga, H.; Heath, E.; Rasmussen, A.; Trock, R.;Johnston, P.; Forastiere, A.; Langmacher, M.; Baylor, A.; Lee, M.; Cullen, K. (1999). Prognostic value of p53, glutathione *S*transferase π, and thymidylate synthase for neoadjuvant cisplatin-based chemotherapy in head and neck cancer, *Clin. Cancer Res., 5*, 4097-4104.
43. Cohn, V.; Lyle, J.; (1966). A fluorometric assay for glutathione, *Anal. Biochem., 14*, 434-440.
44. Hissin, P.; Hilf, R.; (1976). A fluorometric method for the determination of oxidized and reduced glutathione in tissues, *Anal. Biochem., 74*, 214-216.
45. Owens, C.;Belcher, R.; (1965). A colorimetric micro-method for the determination of glutathione, *Biochem. J., 94*, 705-711.
46. Tietze, F.; (1969). Enzymic method for quantitative determination of nanogram amounts of total and oxidized glutathione: application to mammalian blood and other tissues, *Anal. Biochem., 27*, 502-522.
47. Rabenstein, D.; Saetre, R.; (1977). Mercury based electrochemical detector of liquid chromatography for the detection of glutathione and other sulfur-containing compounds, *Anal. Chem., 49*, 1036-1039.
48. Merrills, R.; (1962). An Autoanalytical Method for the Estimation of Adrenaline and Noradrenaline, *Nature, 193*, 988.

49. Kim, H. J.; Hong, J.; Hong, A.; Ham, S.; Lee, J. H.; Kim, J. S. (2008). Cu^{2+}-Induced intermolecular static excimer formation of pyrenealkylamine, *Organic Letters, 10*, 1963-1966.
50. Suresh, M.; Shrivastav, A.; Mishra, S.; Suresh, E.; Das, A. (2008). A rhodamine-based chemosensor that works in the biological system, *Organic Letters, 10*, 3013-3016.
51. Bae, S.; Tae, J. (2007). Rhodamine-hydroxamate-based fluorescent chemosensor for Fe^{III}, *Tetrahedron Letters, 48*, 5389-5392.
52. Palanché, T.; Marmolle, F.; Abdallah, M. A.; Shanzer, A.; Albrecht-Gary, A. (1999). Fluorescent siderophores-based chemosensors: iron(III) quantitative determinations, *Journal of Biological Inorganic Chemistry, 4*, 188-198.
53. Zhang, J.; Badugu, R.; Lakowicz, J. R. (2008). Fluorescence quenching of CdTe nanocrystals by bound gold nanoparticles in aqueous solution, *Plasmonics, 3*, 3-11.
54. Brust, M.; Walker. M.; Bethell, D.; Schiffrin, D. J.; Whyman, R. (1994). Synthesis of thiol-derivatized gold nanoparticles in a 2-phase liquid-liquid system, *J. Chem. Soc. Chem. Commun., 7*, 801–802.
55. Badugu, R.; Kostov, Y.; Rao, G.; Tolosa, L. (2008). Development and application of an excitation ratiometric optical pH sensor for bioprocess monitoring, *Biotech. Prog, in press*.
56. Lakowicz, J. R. *Principles of fluorescence spectroscopy*, 3rd edition, Springer, New York, 2006.

7. Appendix – Auxiliary Figures

7.1. Molecularly Imprinted Polymer for Glutathione

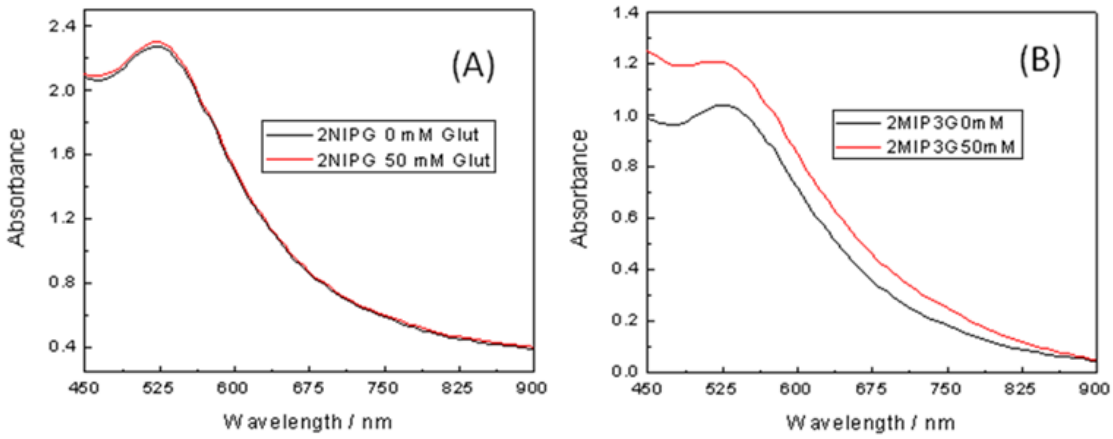

AFig. 1: Plasmon adsorption spectra of gold nanoparticles embedded in non-imprinted (A) and molecularly imprinted polymer (B) in water with 0 and 50 mM glutathione.

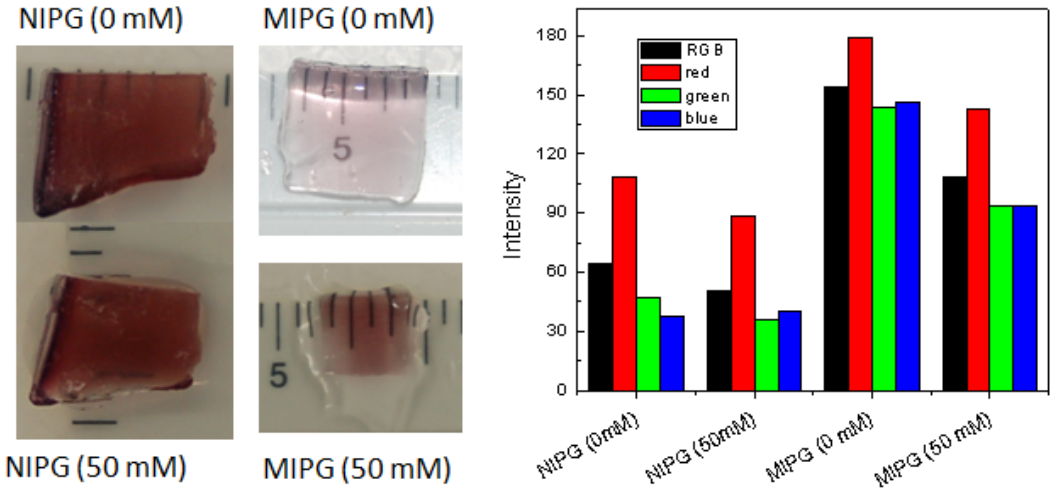

AFig. 2: Photographs of non-imprinted polymer (NIP) and molecular imprinted polymers (MIP) with 0 and 50 mM glutathione (Left). Right side panel shows the corresponding intensities of primary colors with respect to glutathione concentrations obtained from the photographs shown in the left panel.

7.2. Molecularly Imprinted Polymer for Adrenaline

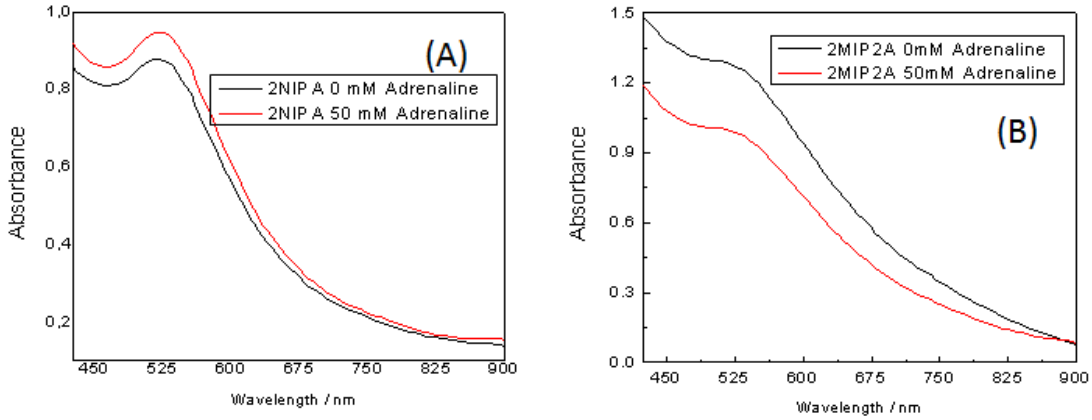

AFig. 3: Plasmon adsorption spectra of gold nanoparticles embedded in non-imprinted (A) and molecularly imprinted polymer (B) in water with 0 and 50 mM adrenaline.

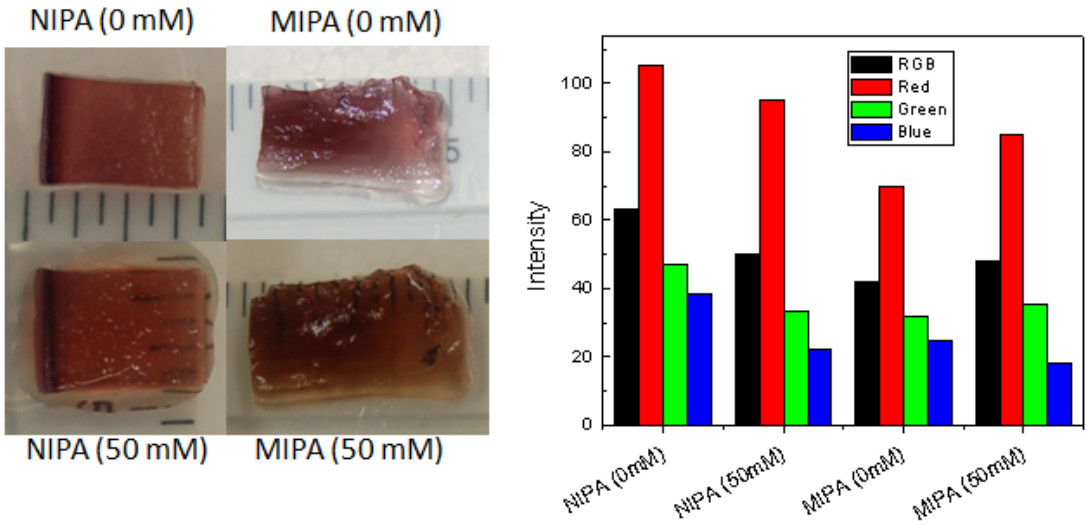

AFig. 4: Photographs of non-imprinted polymer (NIP) and molecular imprinted polymers (MIP) with 0 and 50 mM Adrenaline (Left). Right side panel shows the corresponding intensities of primary colors with respect to adrenaline concentrations obtained from the photographs shown in the left panel.

7.3. NPM labeled NIP and MIP with glutathione

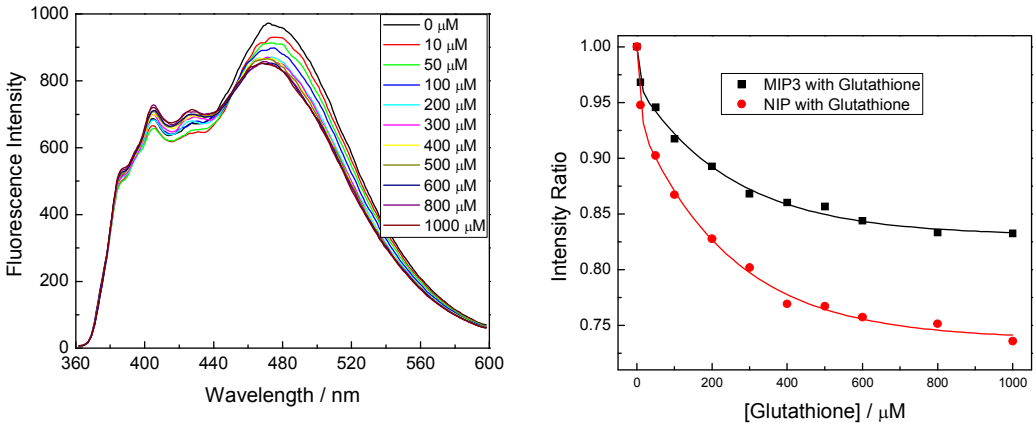

AFig. 5: Fluorescence emission spectra of NPM immobilized and glutathione imprinted polymer in water with increasing concentrations of glutathione (left). The right panel shows the intensity ratio of NPM labeled NIP and MIP plotted against the glutathione concentration. λex = 340 nm.